

Relativistic framework for high-precision GNSS processing in GCRS/BCRS with extension to cislunar space

Slava G. Turyshev, Yoaz E. Bar-Sever and William I. Bertiger
*Jet Propulsion Laboratory, California Institute of Technology,
 4800 Oak Grove Drive, Pasadena, CA 91109-0899, USA*

(Dated: January 13, 2026)

We present an implementation-oriented relativistic modeling framework for high-precision GNSS processing consistent with the IAU-adopted Barycentric and Geocentric Celestial Reference Systems (BCRS/GCRS) and their associated time scales (TCB/TDB and TCG/TT). We derive explicit $\mathcal{O}(c^{-2})$ transformations for position, velocity, and acceleration between TT-compatible GCRS quantities and TDB-compatible BCRS quantities, and provide screened operational forms with conservative remainder bounds that quantify truncation errors in sub-centimeter orbit modeling and retain the term order required by 10^{-16} -class fractional-frequency transfer. We implement a BCRS-native processing option in JPL's GipsyX and validate it via a 24 h round-trip GCRS \rightarrow BCRS propagation-and-transform closure test at the few-mm level, demonstrating internal consistency of the dynamical model and the state transformations. To support emerging Earth–Moon applications, we define a Lunocentric Celestial Reference System (LCRS), its coordinate time (TCL), and a scaled lunar-surface time (TL), and specify a minimal near-rectilinear halo orbit (NRHO)-like regression test that exercises the BCRS \leftrightarrow LCRS transformation chain together with the 1PN barycentric light-time model. End-to-end cislunar navigation performance additionally depends on signal availability and estimation strategy; the present work provides the relativistic reference-frame and time-transfer infrastructure needed to model observables at the centimeter and tens-of-picoseconds level.

CONTENTS

I. Introduction	2
II. Relativistic framework for processing GNSS data	3
A. Coordinate transformations between GCRS and BCRS	3
1. Direct transformations: GCRS \rightarrow BCRS	3
2. Inverse transformations: BCRS \rightarrow GCRS	4
B. Times TT and TDB and related scaling constants	5
1. Relativistic time scales	5
2. Transformations from TT- to TDB-compatible quantities	6
3. Transformations from TDB- to TT-compatible quantities	6
C. Transforming positions, velocity and acceleration	6
1. Preliminary derivations	6
2. Transforming velocity and acceleration	8
D. Practical form for the relevant expressions	8
E. Minimal cislunar regression test: NRHO-like geometry	11
F. Transformation between the proper time and TDB in BCRS	12
1. Direct transformations: TDB \rightarrow proper time	12
2. Inverse transformations: proper time \rightarrow TDB	13
III. BCRS implementation and frame-closure validation for GNSS dynamics	13
A. Equations of motion in the scaled TDB-compatible BCRS	14
1. BCRS metric in the mass monopole approximation	14
2. Equations of motion in BCRS: point-mass approximation	14
3. Light time equation	14
4. Frequency transfer observable at $\mathcal{O}(c^{-3})$	15
B. Equations of motion in the scaled TT-compatible GCRS	15
1. GCRS: Practically-relevant formulation	15
2. Equations of motion in the GCRS	16
3. Transforming equations of motion from GCRS to BCRS	18
4. Considering the gravitational harmonics of the Earth	19

C. Practical implementation and validation	19
IV. Conclusions and next steps	21
Acknowledgments	22
References	22
A. Coordinate Transformation for the Moon System	24
1. Introducing the LCRS	24
2. Transformation between TL and TDB	25
3. Relationships between TL and TT	26
4. Position transformations	27
5. Expressions to transform position, velocity and acceleration	28

I. INTRODUCTION

High-precision spacecraft navigation requires a fully relativistic treatment of both time and space observables [1–3]. Central to this treatment is the choice of an appropriate coordinate reference system. The Barycentric Celestial Reference System (BCRS), with origin at the solar-system barycenter, underlies deep-space applications such as lunar laser ranging (LLR), very long baseline interferometry (VLBI), and the construction of planetary and lunar ephemerides [4]. By contrast, the Geocentric Celestial Reference System (GCRS), centered on Earth’s mass center, is the natural frame for precise orbit determination of GNSS and other Earth-orbiting satellites [2]. Transforming observables between these frames requires inclusion of all $O(c^{-2})$ corrections—gravitational time dilation, velocity-dependent terms, multipolar potential perturbations, and frame-dragging effects—to avoid systematic errors in both timing and positioning.

For Earth-orbiting spacecraft, GCRS-based models incorporate relativistic corrections to the Newtonian equations of motion, including adjustments to central gravitational acceleration and terms arising from Lense-Thirring precession (caused by Earth’s angular momentum), geodesic precession (due to spacetime curvature), and Coriolis effects [5, 6]. These relativistic corrections, while relatively small compared to non-relativistic forces such as atmospheric drag and solar radiation pressure, are critical to achieving the cm-level positional accuracy required for modern navigation systems. Over time, accumulated relativistic errors could cause significant positioning drift in long-duration satellite missions, making it essential to integrate these terms into orbit determination models to prevent systematic errors.

For solar-system navigation beyond Earth orbit it is common to express spacecraft and planetary dynamics in a global barycentric reference system; the IAU-adopted BCRS with coordinate time TCB (or its scaled form TDB) provides the standard realization for modern ephemerides and interplanetary tracking [1, 7, 8]. The mean rate offset between TT and TCB is $L_B = 1.55051976772 \times 10^{-8}$, corresponding to $\simeq 1.34$ ms/day; inconsistent handling of this rate biases modeled one-way and two-way coordinate light-time at the millisecond-per-day level near Earth [8, 9].

As GNSS technology advances with the goal of achieving cm-level positional accuracy, the inclusion of general relativistic corrections in orbit determination models becomes indispensable [10–14]. Modern cm-class GNSS solutions rely on precise orbit and clock products and precise point positioning (PPP) strategies; see, e.g., [15, 16]. These corrections affect multiple aspects of orbit determination, including light-time equations, clock synchronization, station coordinates, and signal propagation delays [2, 17, 18]. For GNSS links, the dominant Shapiro contribution from the Sun is at the few-nanosecond level (meters in range) with mm-level annual modulation, while Earth’s contribution is at the $\lesssim 50$ ps level (Sec. III A 3). Inconsistent handling of the TT–TCB (or TT–TDB) rate introduces a secular ~ 1.34 ms/day bias in coordinate light-time near Earth [8, 9]. Without these corrections, accumulated errors could lead to significant positional offsets, potentially corresponding to meter-level range errors if uncorrected [8].

For interplanetary and lunar applications, navigation observables and dynamical models are often formulated in barycentric coordinates using a first post-Newtonian (1PN) N -body description consistent with the IAU BCRS metric [1, 19]. The secular rate difference between TT and TCB, $L_B - L_G = 1.5505 \times 10^{-8}$, produces a drift of $\simeq 1.34$ ms/day, while the periodic part of TDB – TT reaches $\simeq 1.6$ ms [9]. These time-scale effects correspond to $\mathcal{O}(10^2\text{--}10^5)$ m one-way range-equivalent biases if left untreated, and thus must be handled explicitly (or absorbed consistently) in any mixed GCRS/BCRS estimation problem. At the link level, the 1PN Shapiro delay contributes up to ~ 2.7 ns from the Sun and ~ 40 ps from the Earth for a GNSS MEO signal path [5]; near solar conjunction on interplanetary links it can reach $\mathcal{O}(10\text{--}10^2)$ μs [1]. Accordingly, the key requirement for high-precision processing is an internally consistent set of (i) reference-frame and time-scale transformations, (ii) dynamical models, and (iii) signal-propagation models; the particular choice of integration frame (GCRS vs BCRS) is a design choice rather than a physical necessity.

A consistent treatment across GCRS and BCRS is therefore required for cm/ps-class processing when combining geocentric GNSS models with barycentric ephemerides and relativistic light-time. While standard practice propagates

GNSS spacecraft in the GCRS and transforms states/observables as needed, a BCRS-native processing option becomes convenient when a single estimation pipeline must also accommodate cislunar or interplanetary geometries.

In this work, we report on the implementation of the BCRS framework in JPL’s GipsyX [20], demonstrating mm-level closure results. Specifically, we demonstrate 24 h round-trip GCRS→BCRS propagation-and-transform closure at the few-mm level (Fig. 1), i.e., internal consistency of the dynamical model and state transformations when implemented in GipsyX. The relativistic reference systems used here follow the IAU/IERS conventions and are not new; the contribution of this work is to provide an implementation-oriented, error-budgeted, and software-validated formulation at the levels relevant to modern GNSS processing and its extension to Earth–Moon geometries. In particular, we:

1. Give explicit closed-form $\mathcal{O}(c^{-2})$ transformations for position, velocity, and acceleration between TT-compatible GCRS quantities and TDB-compatible BCRS quantities, with conservative remainder bounds and screening thresholds;
2. Provide an end-to-end GCRS↔BCRS closure experiment in JPL’s GipsyX demonstrating few-mm agreement over 24 h for a GPS-like orbit when using dynamically consistent force models; and
3. Extend the same construction to a Lunicentric Celestial Reference System (LCRS), including its coordinate time (TCL) and a scaled lunar-surface time (TL), together with a minimal NRHO-like regression test that exercises the BCRS↔LCRS transformation chain and the 1PN light-time model.

This paper is structured as follows: In Section II, we present the relativistic framework necessary for processing GNSS data from the BCRS, accounting for current measurement precision. This section addresses the relativistic time scales used in astronomical practice (such as TT, TCG, TCB and TDB) and provides expressions to transform positions, velocities, and accelerations between various practically relevant reference frames. In Section III, we demonstrate the practical implementation of processing GNSS data within the BCRS. This section focuses on applying relativistic corrections, including the transformation of observables between reference frames, and addresses the challenges associated with data analysis when accounting for both the BCRS and GCRS systems. Finally, in Section IV, we summarize the results and discuss their implications for future spacecraft navigation, including applications for extending GNSS capabilities beyond Earth’s vicinity and into the Earth–Moon system. In Appendix A, we introduce and discuss the Lunicentric Celestial Reference System (LCRS) with the associated times TCL and TL, which is essential for accurately modeling GNSS receivers operating in cislunar space, where gravitational and relativistic effects must be well-modeled.

II. RELATIVISTIC FRAMEWORK FOR PROCESSING GNSS DATA

A. Coordinate transformations between GCRS and BCRS

1. Direct transformations: GCRS → BCRS

According to the IAU conventions, the GCRS is realized by the geocentric metric tensor G_{mn} in coordinates (T, \mathbf{X}) , where $T \equiv \text{TCG}$ denotes Geocentric Coordinate Time [7]. Following the approach of [8, 21], we express G_{mn} to the order required for modern GNSS timing applications. Since current GNSS clocks reach fractional frequency stabilities of order 3×10^{-15} , the recommended transformations¹ from the GCRS ($T = \text{TCG}$, \mathbf{X}) to the BCRS ($t = \text{TCB}$, $\mathbf{r}_E = \mathbf{x} - \mathbf{x}_E(t)$) for GNSS data processing then take the form:

$$T = t - c^{-2} \left\{ \int_{t_0}^t \left(\frac{1}{2} v_E^2 + \sum_{B \neq E} \frac{GM_B}{r_{BE}} \right) dt + (\mathbf{v}_E \cdot \mathbf{r}_E) \right\} + \mathcal{O}\left(1.10 \times 10^{-16}(t - t_0)\right), \quad (1)$$

$$\mathbf{X} = \mathbf{r}_E + c^{-2} \left\{ \frac{1}{2} (\mathbf{v}_E \cdot \mathbf{r}_E) \mathbf{v}_E + \sum_{B \neq E} \frac{GM_B}{r_{BE}} \mathbf{r}_E + (\mathbf{a}_E \cdot \mathbf{r}_E) \mathbf{r}_E - \frac{1}{2} r_E^2 \mathbf{a}_E \right\} + \mathcal{O}\left(1.28 \times 10^{-12} \text{ m}\right), \quad (2)$$

where \mathbf{x}_E and $\mathbf{v}_E = d\mathbf{x}_E/dt$ being the Earth’s position and velocity vectors in the BCRS, with their magnitudes known to be $x_E = |\mathbf{x}_E| \equiv \text{AU} \simeq 1.49597870700 \times 10^{11} \text{ m}$, and $v_E = |\mathbf{v}_E| = 29784.7 \text{ m/s}$, see Table II. Here t_0 is an arbitrary reference epoch (e.g., J2000) that fixes the integration constant in the time transformation, and $T_0 \equiv T(t_0)$ denotes

¹ The notational conventions employed in this paper are those used in [1, 22]. Letters from the second half of the Latin alphabet, $m, n, \dots = 0\dots3$ denote spacetime indices. Greek letters $\alpha, \beta, \dots = 1\dots3$ denote spatial indices. The metric γ_{mn} is that of Minkowski spacetime with $\gamma_{mn} = \text{diag}(+1, -1, -1, -1)$ in the Cartesian representation. We employ the Einstein summation convention with indices being lowered or raised using γ_{mn} . We use powers of G and negative powers of c as bookkeeping devices for order terms.

the corresponding TCG epoch. All modeled observables depend only on time differences, so the choice of t_0 cancels provided it is used consistently throughout the transformation chain. Note that in their most accurate form (see [7]), the time transformations (1) also include terms $\propto \mathcal{O}(c^{-4})$. The uncertainty in (1) comes from the omitted $\mathcal{O}(c^{-4})$ terms behaving as $\sim c^{-4}(-\frac{1}{8}v_E^2 - \frac{3}{2}v_E^2 GM_S/r_E + \frac{1}{2}(GM_S/r_E)^2) \lesssim -1.10 \times 10^{-16} = -9.50$ ps/d.

Consider a GPS spacecraft at an altitude of $h_{\text{GPS}} = 20\,200$ km, thus its distance from the origin of the GCRS is $r_{\text{GPS}} = R_E + h_{\text{GPS}} = 26\,578$ km and the geocentric velocity is $v_{\text{GPS}} \simeq \sqrt{GM_E/r_{\text{GPS}}} \simeq 3\,872.64$ m/s. Then, the c^{-2} terms under the integral in (1) were evaluated to contribute up to $c^{-2}(\frac{1}{2}v_E^2 + \sum_{B \neq E} GM_B/r_{BE}) \simeq c^{-2}(\frac{3}{2}GM_S/AU + GM_M/r_{EM}) \simeq 1.48061 \times 10^{-8}$, while position-dependent term has the magnitude of $c^{-2}(\mathbf{v}_E \cdot \mathbf{r}_E) \lesssim c^{-2}v_E r_{\text{GPS}} \approx 8.81 \times 10^{-6} \text{ s} = 8.81 \mu\text{s}$. In (2), the velocity-dependent term $c^{-2}\frac{1}{2}(\mathbf{v}_E \cdot \mathbf{r}_E)\mathbf{v}_E \simeq c^{-2}\frac{1}{2}v_E^2 r_{\text{GPS}} \simeq 13.12$ cm reflects the Lorentz contraction, while the term $c^{-2}\sum_{B \neq E}(GM_B/r_{BE})\mathbf{r}_E \simeq c^{-2}(GM_S/AU + GM_M/r_{EM})r_{\text{GPS}} \simeq 26.24$ cm corresponds to an isotropic rescaling of length due to the external potential. Both terms are significant and must be included in the model.

The acceleration-dependent terms in (2) may contribute up to 2.68×10^{-6} m at a ground station and 4.66×10^{-5} m at r_{GPS} . Although these offsets are small, they become significant when comparing spacecraft accelerations in the BCRS and the GCRS. The dominant uncertainty in (2) stems from the neglected solar quadrupole moment, $J_2 = 2.25 \times 10^{-7}$ [23, 24], which induces corrections of order $c^{-2}w_{2,S}(t, \mathbf{x})\mathbf{r}_E \simeq c^{-2}(GM_S J_2 R_S^2/AU^3)R_{\text{GPS}} \sim 1.28 \times 10^{-12}$ m, a value that is entirely negligible and therefore serves as a conservative error bound.

2. Inverse transformations: BCRS \rightarrow GCRS

To compare the relativistic description of spacecraft acceleration across different coordinate reference systems, we also require the inverse transformations. Accordingly, the transformations from the BCRS back to the GCRS, inverse to (1)–(2), is obtained by noting that the relativistic time transformation at the GCRS origin ($\mathbf{X} = 0$) is given as

$$T = t^* - \frac{1}{c^2} \int_{t_0}^{t^*} \left(\frac{1}{2}v_E^2 + \sum_{B \neq E} \frac{GM_B}{r_{BE}} \right) dt + \mathcal{O}\left(1.10 \times 10^{-16}(t^* - t_0)\right). \quad (3)$$

and the TCG representation of the motion of the Earth with respect to the BCRS given as below

$$\bar{\mathbf{x}}_E(T) = \mathbf{x}_E(t^*), \quad (4)$$

These relations can be obtained either numerically or analytically. In the case of the direct transformations, (1)–(2), one must evaluate the integral in (1) by numerical quadrature or, where possible, in closed form. For the inverse transformations, the time transformations $t^* = t^*(T)$ is found by inverting (3), again using either numerical or analytical methods. Here, (3) follows directly from applying the GCRS time transformation, (1), at the geocenter ($\mathbf{X} = 0$).

We can connect the Earth's center world line, $\mathbf{x}_E(t)$, to an observer's world line, $\mathbf{x}(t)$, using a space-time curve that is orthogonal to both world lines. Note that in data-processing programs the relevant coordinate differences are not simply $\Delta \mathbf{r}$, but rather the simultaneous barycentric differences $\Delta \mathbf{r} = \mathbf{x}(t^*) - \mathbf{x}_E(t^*)$ evaluated at a common barycentric coordinate time t^* .

Accordingly, in the inverse transformations of a geocentric position vector \mathbf{X} from the GCRS (compatible with TCG, TAI, or TT for ground stations) to the solar system barycentric frame (compatible with TDB), one must account for the Lorentz contraction of \mathbf{X} and make relativistic adjustments to the scale of \mathbf{X} , as illustrated below:

$$t = T + \frac{1}{c^2} \left\{ \int_{T_0}^T \left(\frac{1}{2}v_E^2 + \sum_{B \neq E} \frac{GM_B}{r_{BE}} \right) dT + (\mathbf{v}_E \cdot \mathbf{X}) \right\} + \mathcal{O}\left(1.10 \times 10^{-16}\right)(T - T_0), \quad (5)$$

$$\mathbf{r}_E = \mathbf{X} - c^{-2} \left\{ \frac{1}{2}(\mathbf{v}_E \cdot \mathbf{X})\mathbf{v}_E + \sum_{B \neq E} \frac{GM_B}{r_{BE}} \mathbf{X} + (\mathbf{a}_E \cdot \mathbf{X})\mathbf{X} - \frac{1}{2}X^2 \mathbf{a}_E \right\} + \mathcal{O}\left(1.28 \times 10^{-12} \text{ m}\right). \quad (6)$$

Here T_0 is the conventional reference epoch used in the IAU scaling definitions (see Sec. IIB and Table 1); the corresponding TCB epoch at the geocenter is $t_0 = t^*(T_0)$.

As a result, we now have both direct (1)–(2) and inverse (5)–(6) coordinate transformations between BCRS and GCRS, which are provided with accuracy sufficient for processing GNSS data from either frame. Note that a similar set of transformations, albeit without acceleration-dependent terms, has been implemented for processing LLR data, as discussed in [25]. Special attention must be given when dealing with either ground stations or Earth-orbiting spacecraft, as the coordinates \mathbf{X} will differ [21]. Specifically, terms proportional to $1/c^4$ in the time transformations (1) and (5) are necessary if a frequency transfer accuracy of approximately 1.0×10^{-16} is required, and acceleration-dependent terms in position transformations (2) and (6) are needed for positional accuracy within a few millimeters.

TABLE I. Reference time-scale constants and implied mean rates (IAU/IERS defining constants used in this work).

Symbol	Definition	Value (s/s)	Mean rate per day	Note
L_G	$dTT/dTCG = 1 - L_G$	$6.969\,290\,134 \times 10^{-10}$	$60.2146 \mu\text{s d}^{-1}$	IAU 2000 B1.9
L_C	$\langle dTCG/dTCB \rangle = 1 - L_C$	$1.480\,826\,867\,41 \times 10^{-8}$	$1.279\,434 \text{ ms d}^{-1}$	IAU 2000 B1.5
L_B	$1 - L_B = (1 - L_G)(1 - L_C)$	$1.550\,519\,767\,72 \times 10^{-8}$	$1.339\,649 \text{ ms d}^{-1}$	IAU 2006/2009
L_L	$dTL/dTCL = 1 - L_L$	$3.1390541 \times 10^{-11}$	$2.712143 \mu\text{s d}^{-1}$	this work, Eq. (A5)
L_H	$\langle dTCL/dTCB \rangle = 1 - L_H$	1.4825362×10^{-8}	$1.280\,911 \text{ ms d}^{-1}$	this work, Eq. (A8)
L_M	$\langle dTL/dTCB \rangle = 1 - L_M$	$1.485675294 \times 10^{-8}$	$1.283\,624 \text{ ms d}^{-1}$	this work, Eq. (A10)

B. Times TT and TDB and related scaling constants

1. Relativistic time scales

To compare clocks following different world-lines in the solar system one needs to account for the differences in relevant dynamical environment. We first consider the relationship between TT and TCG. TT was defined by IAU Resolution A4 (1991) [26] as: ‘a time scale differing from TCG by a constant rate, with the unit of measurement of TT chosen so that it matches the SI second on the geoid.’ According to the transformation between proper and coordinate time, this constant rate is expressed as

$$\frac{dTT}{dTCG} = 1 - \frac{1}{c^2} W_g = 1 - L_G, \quad (7)$$

where W_g is the combined gravitational and rotational potential on the geoid, determined as $W_g = (62636856.0 \pm 0.5) \text{ m}^2\text{s}^{-2}$ [27]. The IAU value for L_G is $6.969\,290\,134 \times 10^{-10} \approx 60.2$ microseconds/day ($\mu\text{s/d}$), a defining constant as set by IAU 2000 Resolution B1.9, Table 1.1 in [5].

According to the IAU Resolutions [28], instead of coordinate time $T = \text{TCG}$, spatial coordinates \mathbf{X} and mass factors $(GM)_{\text{TCG}}$ related to GCRS, the following scaling of these quantities is used [8, 21]

$$\text{TT} = \text{TCG} - L_G(\text{TCG} - T_0), \quad \mathbf{X}_{\text{TT}} = (1 - L_G)\mathbf{X}_{\text{TCG}}, \quad (GM)_{\text{TT}} = (1 - L_G)(GM)_{\text{TCG}}, \quad (8)$$

where T_0 is the conventional reference epoch used in the IAU scaling definitions; in this work we adopt $T_0 = 2443144.5003725$ JD, as in Eq. (11).

Another constant L_C removes the constant rate between TCG and TCB. It is determined as the long time average of the rate computed from the full post-Newtonian version of (5) accurate to $\mathcal{O}(c^{-4})$ (see [8]):

$$\left\langle \frac{dTCG}{dTCB} \right\rangle = 1 - L_C. \quad (9)$$

According to the IAU 2000 Resolution B1.5, $L_C = 1.480\,826\,867\,41 \times 10^{-8} \pm 2 \times 10^{-17} \approx 1.279\,434\,4 \text{ ms/d} \pm 1.7 \text{ ps/d}$, introducing it as a fundamental constant (refer to Table 1.1 in [5]).

The IAU 2000 Resolution B1.5, recommended the following relationship between the constants L_B , L_G , and L_C :

$$\left\langle \frac{dTT}{dTCB} \right\rangle = \left(\frac{dTT}{dTCG} \right) \left\langle \frac{dTCG}{dTCB} \right\rangle \quad \Rightarrow \quad 1 - L_B = (1 - L_G)(1 - L_C), \quad (10)$$

where L_B is determined as $L_B = L_G + L_C - L_G L_C = 1.550\,519\,767\,72 \times 10^{-8} \approx 1.34 \text{ ms/d}$.

Finally, TDB is a timescale rescaled from TCB, as defined by IAU 2006 Resolution B3 and IAU 2009 Resolution 3 [5, 29], given by the following set of expressions:

$$\text{TDB} = \text{TCB} - L_B(\text{TCB} - T_0) + \text{TDB}_0, \quad \mathbf{x}_{\text{TDB}} = (1 - L_B)\mathbf{x}_{\text{TCB}}, \quad (GM)_{\text{TDB}} = (1 - L_B)(GM)_{\text{TCB}}, \quad (11)$$

where, the defining constants $L_B = 1.550519768 \times 10^{-8}$, $T_0 = 2443144.5003725$ JD, and $\text{TDB}_0 = -65.5 \mu\text{s}$, match those used in the JPL DE405 ephemeris [30]. This ensures that TDB advances at the same rate as TT at the geocenter. The offset TDB_0 is chosen to align with the standard (TDB – TT) relation [31], which implies that TDB is not synchronized with TT, TCG, or TCB at 1977-01-01 00:00:32.184 TAI, at the geocenter (see discussion in [8, 21]).

2. Transformations from TT- to TDB-compatible quantities

To process the GNSS data, one needs an expression for the time transformations between GCRS (TT, \mathbf{X}_{TT}) and BCRS (TDB, $(\mathbf{r}_{\text{E}})_{\text{TDB}} = (\mathbf{x} - \mathbf{x}_{\text{E}}(t))_{\text{TDB}}$). By applying the relevant scaling relationships specified in (8) and (11), and introducing $(\mathbf{v}_{\text{E}} \cdot \mathbf{r}_{\text{E}})_{\text{TDB}} = (\mathbf{v}_{\text{E}} \cdot (\mathbf{r}_{\text{E}})_{\text{TDB}})$, we have relationships in terms of the TDB-compatible quantities (see details in [21])

$$\begin{aligned} \text{TT} &= \text{TDB} - \text{TDB}_0 + L_{\text{C}} \left(\text{TDB} - \text{T}_0 - \text{TDB}_0 \right) - \\ &- c^{-2} \left\{ \int_{\text{T}_0 + \text{TDB}_0}^{\text{TDB}} \left(\frac{1}{2} v_{\text{E}}^2 + \sum_{\text{B} \neq \text{E}} \frac{GM_{\text{B}}}{r_{\text{BE}}} \right) dt + (\mathbf{v}_{\text{E}} \cdot \mathbf{r}_{\text{E}}) \right\}_{\text{TDB}} + \mathcal{O}(2.19 \times 10^{-16}) (\text{TDB} - \text{T}_0 - \text{TDB}_0), \end{aligned} \quad (12)$$

$$\mathbf{X}_{\text{TT}} = (1 + L_{\text{C}}) \mathbf{r}_{\text{ETDB}} + c^{-2} \left\{ \frac{1}{2} (\mathbf{v}_{\text{E}} \cdot \mathbf{r}_{\text{E}}) \mathbf{v}_{\text{E}} + \sum_{\text{B} \neq \text{E}} \frac{GM_{\text{B}}}{r_{\text{BE}}} \mathbf{r}_{\text{E}} + (\mathbf{a}_{\text{E}} \cdot \mathbf{r}_{\text{E}}) \mathbf{r}_{\text{E}} - \frac{1}{2} r_{\text{E}}^2 \mathbf{a}_{\text{E}} \right\}_{\text{TDB}} + \mathcal{O}(5.83 \times 10^{-9} \text{ m}). \quad (13)$$

Note that the errors in (12) are determined by the omitted products of the L_{C}^2 term. If included, the error would be $\sim \mathcal{O}(1.46 \times 10^{-16})$, resulting from the product of L_{C} and the external gravitational potential. Similarly, the error in (13) is set by the omitted term $L_{\text{C}}^2 (\mathbf{r}_{\text{E}})_{\text{TDB}} \simeq \mathcal{O}(5.83 \times 10^{-9} \text{ m})$.

3. Transformations from TDB- to TT-compatible quantities

Similarly, we can develop inverse transformations for transitioning from TDB-compatible to TT-compatible quantities. For this, we use expressions for the transforming from BCRS to GCRS given by (5)–(6). Then, applying the scaling relationships (8) and (11), we have:

$$\text{TDB} = (1 - L_{\text{C}}) \text{TT} + L_{\text{C}} \text{T}_0 + \text{TDB}_0 + \frac{1}{c^2} \left\{ \int_{\text{T}_0}^{\text{TT}} \left(\frac{1}{2} v_{\text{E}}^2 + \sum_{\text{B} \neq \text{E}} \frac{GM_{\text{B}}}{r_{\text{BE}}} \right) dt + (\mathbf{v}_{\text{E}} \cdot \mathbf{X}) \right\}_{\text{TT}} + \mathcal{O}(1.46 \times 10^{-16}) (\text{TT} - \text{T}_0), \quad (14)$$

$$(\mathbf{r}_{\text{E}})_{\text{TDB}} = (1 - L_{\text{C}}) \mathbf{X}_{\text{TT}} - c^{-2} \left\{ \frac{1}{2} (\mathbf{v}_{\text{E}} \cdot \mathbf{X}) \mathbf{v}_{\text{E}} + \sum_{\text{B} \neq \text{E}} \frac{GM_{\text{B}}}{r_{\text{BE}}} \mathbf{X} + (\mathbf{a}_{\text{E}} \cdot \mathbf{X}) \mathbf{X} - \frac{1}{2} X^2 \mathbf{a}_{\text{E}} \right\}_{\text{TT}} + \mathcal{O}(5.83 \times 10^{-9} \text{ m}). \quad (15)$$

Note that the error in (14) is set by the product of L_{C} and the external gravitational potential. Similar to (13), the errors in (15) are due to omitted $L_{\text{C}}^2 \mathbf{X}_{\text{TT}} \simeq 5.83 \times 10^{-9} \text{ m}$ term.

Result (14) yields the following useful derivative:

$$\frac{d\text{TDB}}{d\text{TT}} = 1 - L_{\text{C}} + c^{-2} \left\{ \frac{1}{2} v_{\text{E}}^2 + \sum_{\text{B} \neq \text{E}} \frac{GM_{\text{B}}}{r_{\text{BE}}} + (\mathbf{a}_{\text{E}} \cdot \mathbf{X}) + (\mathbf{v}_{\text{E}} \cdot \dot{\mathbf{X}}) \right\}_{\text{TT}} + \mathcal{O}(1.46 \times 10^{-16}). \quad (16)$$

Now we have all the expressions needed to establish the transformation rules for velocities and accelerations.

C. Transforming positions, velocity and acceleration

1. Preliminary derivations

We now present the transformation required for the TT-compatible GCRS position vector \mathbf{X}_{TT} , velocity $\mathbf{V}_{\text{TT}} = \dot{\mathbf{X}}_{\text{TT}} = d\mathbf{X}/d\text{TT}$, and acceleration $\mathbf{A}_{\text{TT}} = \ddot{\mathbf{X}}_{\text{TT}} = d\dot{\mathbf{X}}_{\text{TT}}/d\text{TT} = d^2\mathbf{X}/d\text{TT}^2$. These transformations will convert these measurements to the BCRS with TDB-compatible position $(\mathbf{r}_{\text{E}})_{\text{TDB}} = (\mathbf{x} - \mathbf{x}_{\text{E}})_{\text{TDB}}$, velocity $(\dot{\mathbf{r}}_{\text{E}})_{\text{TDB}} = d(\mathbf{r}_{\text{E}})_{\text{TDB}}/d\text{TDB} = (\mathbf{v} - \mathbf{v}_{\text{E}})_{\text{TDB}}$, and acceleration $(\ddot{\mathbf{r}}_{\text{E}})_{\text{TDB}} = d(\dot{\mathbf{r}}_{\text{E}})_{\text{TDB}}/d\text{TDB} = d^2(\mathbf{r}_{\text{E}})_{\text{TDB}}/d\text{TDB}^2 = (\mathbf{a} - \mathbf{a}_{\text{E}})_{\text{TDB}}$.

We begin with the position transformation that is given by (15), expressing it, for convenience, as below

$$(\mathbf{r}_{\text{E}})_{\text{TDB}} = (\mathbf{x} - \mathbf{x}_{\text{E}})_{\text{TDB}} = \mathbf{X}_{\text{TT}} - \Delta \mathbf{X}_{\text{TT}}, \quad (17)$$

where the corrective term $\Delta \mathbf{X}_{\text{TT}}$ is of the order of $\mathcal{O}(c^{-2})$ and is given as

$$\Delta \mathbf{X}_{\text{TT}} = L_{\text{C}} \mathbf{X}_{\text{TT}} + c^{-2} \left\{ \frac{1}{2} (\mathbf{v}_{\text{E}} \cdot \mathbf{X}) \mathbf{v}_{\text{E}} + \gamma U_{\text{ext}} \mathbf{X} + (\mathbf{a}_{\text{E}} \cdot \mathbf{X}) \mathbf{X} - \frac{1}{2} X^2 \mathbf{a}_{\text{E}} \right\}_{\text{TT}} + \mathcal{O}(5.83 \times 10^{-9} \text{ m}), \quad (18)$$

where, for convenience, we use

$$U_{\text{ext}} \equiv \sum_{\text{B} \neq \text{E}} \frac{GM_{\text{B}}}{r_{\text{BE}}} + \mathcal{O}(c^{-2}). \quad (19)$$

Note that in (18) we also brought in the PPN parameter γ as in [1]. We evaluate derivatives along TT unless noted: $\dot{U}_{\text{ext}} = -\sum_{\text{B} \neq \text{E}} GM_{\text{B}} [(\mathbf{v}_{\text{B}} - \mathbf{v}_{\text{E}}) \cdot (\mathbf{x}_{\text{B}} - \mathbf{x}_{\text{E}})] / r_{\text{BE}}^3$ and \ddot{U}_{ext} analogously by differentiating once more; see (27)–(28). We explicitly retain the PPN parameter γ (with $\gamma = 1$ in general relativity) to make clear which terms in the GCRS \leftrightarrow BCRS state transformations would change in a PPN analysis; all numerical evaluations in this work set $\gamma = 1$.

Similarly, recognizing from (15) that $\mathbf{r}_{\text{ETDB}} = \mathbf{X}_{\text{TT}} + \mathcal{O}(c^{-2})$ and $\dot{\mathbf{r}}_{\text{ETDB}} = \dot{\mathbf{X}}_{\text{TT}} + \mathcal{O}(c^{-2})$ we present

$$\frac{dT_{\text{T}}}{dT_{\text{DB}}} = 1 + L_{\text{C}} - c^{-2} \left\{ \frac{1}{2} v_{\text{E}}^2 + U_{\text{ext}} + (\mathbf{a}_{\text{E}} \cdot \mathbf{X}) + (\mathbf{v}_{\text{E}} \cdot \dot{\mathbf{X}}) \right\}_{\text{TT}} + \mathcal{O}(2.19 \times 10^{-16}). \quad (20)$$

Numerically at the geocenter, $GM_{\odot}/\text{AU} \simeq 8.87 \times 10^8 \text{ m}^2/\text{s}^2$ while $GM_{\text{M}}/r_{\text{EM}} \simeq 1.28 \times 10^4 \text{ m}^2/\text{s}^2$; thus the solar term dominates U_{ext} by $\sim 7 \times 10^4$, with other planetary contributions smaller still.

We can now develop the time derivatives of $(\mathbf{r}_{\text{E}})_{\text{TDB}}$:

$$(\dot{\mathbf{r}}_{\text{E}})_{\text{TDB}} = \frac{d(\mathbf{r}_{\text{E}})_{\text{TDB}}}{dT_{\text{DB}}} \equiv (\dot{\mathbf{x}} - \mathbf{v}_{\text{E}})_{\text{TDB}}, \quad (\ddot{\mathbf{r}}_{\text{E}})_{\text{TDB}} = \frac{d^2(\mathbf{r}_{\text{E}})_{\text{TDB}}}{dT_{\text{DB}}^2} \equiv (\ddot{\mathbf{x}} - \mathbf{a}_{\text{E}})_{\text{TDB}}. \quad (21)$$

For that, similarly to [32] and using expressions (17)–(18), we have

$$\frac{d(\mathbf{r}_{\text{E}})_{\text{TDB}}}{dT_{\text{DB}}} = \frac{d\mathbf{X}_{\text{TT}}}{dT_{\text{T}}} \frac{dT_{\text{T}}}{dT_{\text{DB}}} - \frac{d\Delta\mathbf{X}_{\text{TT}}}{dT_{\text{T}}} \frac{dT_{\text{T}}}{dT_{\text{DB}}}, \quad (22)$$

$$\frac{d^2(\mathbf{r}_{\text{E}})_{\text{TDB}}}{dT_{\text{DB}}^2} = \frac{d^2\mathbf{X}_{\text{TT}}}{dT_{\text{T}}^2} \left(\frac{dT_{\text{T}}}{dT_{\text{DB}}} \right)^2 + \frac{d\mathbf{X}_{\text{TT}}}{dT_{\text{T}}} \frac{d^2T_{\text{T}}}{dT_{\text{DB}}^2} - \frac{d^2\Delta\mathbf{X}_{\text{TT}}}{dT_{\text{T}}^2} \left(\frac{dT_{\text{T}}}{dT_{\text{DB}}} \right)^2 - \frac{d\Delta\mathbf{X}_{\text{TT}}}{dT_{\text{T}}} \frac{d^2T_{\text{T}}}{dT_{\text{DB}}^2}. \quad (23)$$

From (20), we see that $dT_{\text{T}}/dT_{\text{DB}} = 1 + \mathcal{O}(c^{-2})$. In addition, $\Delta\mathbf{X}_{\text{TT}}$ is of the order of $\mathcal{O}(c^{-2})$. Given this, we may simplify (22) and (23), as below

$$\frac{d(\mathbf{r}_{\text{E}})_{\text{TDB}}}{dT_{\text{DB}}} = \frac{d\mathbf{X}_{\text{TT}}}{dT_{\text{T}}} \frac{dT_{\text{T}}}{dT_{\text{DB}}} - \frac{d\Delta\mathbf{X}_{\text{TT}}}{dT_{\text{T}}} + \mathcal{O}(c^{-4}), \quad (24)$$

$$\frac{d^2(\mathbf{r}_{\text{E}})_{\text{TDB}}}{dT_{\text{DB}}^2} = \frac{d^2\mathbf{X}_{\text{TT}}}{dT_{\text{T}}^2} \left(\frac{dT_{\text{T}}}{dT_{\text{DB}}} \right)^2 + \frac{d\mathbf{X}_{\text{TT}}}{dT_{\text{T}}} \frac{d^2T_{\text{T}}}{dT_{\text{DB}}^2} - \frac{d^2\Delta\mathbf{X}_{\text{TT}}}{dT_{\text{T}}^2} + \mathcal{O}(c^{-4}). \quad (25)$$

Using (20), we have

$$\frac{dT_{\text{T}}}{dT_{\text{DB}}} = 1 + L_{\text{C}} - c^{-2} \left\{ \frac{1}{2} v_{\text{E}}^2 + U_{\text{ext}} + (\mathbf{a}_{\text{E}} \cdot \mathbf{X}) + (\mathbf{v}_{\text{E}} \cdot \dot{\mathbf{X}}) \right\}_{\text{TT}} + \mathcal{O}(2.19 \times 10^{-16}), \quad (26)$$

$$\left(\frac{dT_{\text{T}}}{dT_{\text{DB}}} \right)^2 = 1 + 2L_{\text{C}} - c^{-2} \left\{ v_{\text{E}}^2 + 2U_{\text{ext}} + 2(\mathbf{a}_{\text{E}} \cdot \mathbf{X}) + 2(\mathbf{v}_{\text{E}} \cdot \dot{\mathbf{X}}) \right\}_{\text{TT}} + \mathcal{O}(4.38 \times 10^{-16}), \quad (27)$$

$$\frac{d^2T_{\text{T}}}{dT_{\text{DB}}^2} = -c^{-2} \left\{ (\mathbf{v}_{\text{E}} \cdot \mathbf{a}_{\text{E}}) + \dot{U}_{\text{ext}} + (\dot{\mathbf{a}}_{\text{E}} \cdot \mathbf{X}) + 2(\mathbf{a}_{\text{E}} \cdot \dot{\mathbf{X}}) + (\mathbf{v}_{\text{E}} \cdot \ddot{\mathbf{X}}) \right\}_{\text{TT}} + \mathcal{O}(2.91 \times 10^{-23} \text{ s}^{-1}), \quad (28)$$

where the error in $d^2T_{\text{T}}/dT_{\text{DB}}^2$ is set by the magnitude of the omitted c^{-4} terms (12), see [21].

In addition, from (18), we compute

$$\begin{aligned} \frac{d\Delta\mathbf{X}_{\text{TT}}}{dT_{\text{T}}} &= L_{\text{C}} \dot{\mathbf{X}}_{\text{TT}} + c^{-2} \left\{ \frac{1}{2} \left((\mathbf{a}_{\text{E}} \cdot \mathbf{X}) + (\mathbf{v}_{\text{E}} \cdot \dot{\mathbf{X}}) \right) \mathbf{v}_{\text{E}} + \left(\frac{1}{2} (\mathbf{v}_{\text{E}} \cdot \mathbf{X}) - (\mathbf{X} \cdot \dot{\mathbf{X}}) \right) \mathbf{a}_{\text{E}} + \left((\mathbf{a}_{\text{E}} \cdot \mathbf{X}) + \gamma U_{\text{ext}} \right) \dot{\mathbf{X}} \right. \\ &\quad \left. + \left((\dot{\mathbf{a}}_{\text{E}} \cdot \mathbf{X}) + (\mathbf{a}_{\text{E}} \cdot \dot{\mathbf{X}}) + \gamma \dot{U}_{\text{ext}} \right) \mathbf{X} - \frac{1}{2} X^2 \dot{\mathbf{a}}_{\text{E}} \right\}_{\text{TT}} + \mathcal{O}(8.49 \times 10^{-13} \text{ m/s}), \end{aligned} \quad (29)$$

where the errors in (29) are set by the term $L_{\text{C}}^2 (\mathbf{r}_{\text{E}})_{\text{TDB}} = L_{\text{C}}^2 \mathbf{X}_{\text{TT}} + \mathcal{O}(c^{-2}) \simeq 5.83 \times 10^{-9} \text{ m}$ omitted in (29), that yields $L_{\text{C}}^2 \dot{\mathbf{X}}_{\text{TT}} \simeq 8.49 \times 10^{-13} \text{ m/s}$ for a MEO orbiter. Also, $\dot{U}_{\text{ext}} = dU_{\text{ext}}/dT_{\text{T}} + \mathcal{O}(c^{-2})$ has the form

$$\dot{U}_{\text{ext}} \equiv \frac{dU_{\text{ext}}}{dT_{\text{T}}} = - \sum_{\text{B} \neq \text{E}} \frac{GM_{\text{B}} ((\mathbf{v}_{\text{B}} - \mathbf{v}_{\text{E}}) \cdot (\mathbf{x}_{\text{B}} - \mathbf{x}_{\text{E}}))}{r_{\text{BE}}^3} + \mathcal{O}(c^{-2}), \quad (30)$$

with GM_B , \mathbf{r}_B and \mathbf{v}_B being the mass parameter and barycentric position and velocity vectors of body B, E is the index for Earth and r_{BE} is the geocentric range of body B and $r_{BE} = |\mathbf{x}_B - \mathbf{x}_E|$.

Finally, we use (29) to compute

$$\begin{aligned} \frac{d^2 \Delta \mathbf{X}_{TT}}{dTT^2} &= L_C \ddot{\mathbf{X}}_{TT} + c^{-2} \left\{ \frac{1}{2} \left((\dot{\mathbf{a}}_E \cdot \mathbf{X}) + 2(\mathbf{a}_E \cdot \dot{\mathbf{X}}) + (\mathbf{v}_E \cdot \ddot{\mathbf{X}}) \right) \mathbf{v}_E + \left((\mathbf{a}_E \cdot \mathbf{X}) + (\mathbf{v}_E \cdot \dot{\mathbf{X}}) - (\dot{\mathbf{X}} \cdot \dot{\mathbf{X}}) - (\mathbf{X} \cdot \ddot{\mathbf{X}}) \right) \mathbf{a}_E + \right. \\ &+ \left(\frac{1}{2} (\mathbf{v}_E \cdot \mathbf{X}) - 2(\mathbf{X} \cdot \dot{\mathbf{X}}) \right) \dot{\mathbf{a}}_E + \left(\gamma \ddot{U}_{\text{ext}} + (\ddot{\mathbf{a}}_E \cdot \mathbf{X}) + 2(\dot{\mathbf{a}}_E \cdot \dot{\mathbf{X}}) + (\mathbf{a}_E \cdot \ddot{\mathbf{X}}) \right) \mathbf{X} + \\ &+ \left. 2 \left(\gamma \dot{U}_{\text{ext}} + (\dot{\mathbf{a}}_E \cdot \mathbf{X}) + (\mathbf{a}_E \cdot \dot{\mathbf{X}}) \right) \dot{\mathbf{X}} + \left(\gamma U_{\text{ext}} + (\mathbf{a}_E \cdot \mathbf{X}) \right) \ddot{\mathbf{X}} - \frac{1}{2} X^2 \ddot{\mathbf{a}}_E \right\}_{TT} + \mathcal{O} \left(1.24 \times 10^{-16} \text{ m/s}^2 \right), \quad (31) \end{aligned}$$

where the errors in (31) are set by the omitted term $L_C^2 (\mathbf{r}_E)_{\text{TDB}} = L_C^2 \mathbf{X}_{TT} + \mathcal{O}(c^{-2}) \simeq 5.83 \times 10^{-9} \text{ m}$ omitted in (29), that yields $L_C^2 \ddot{\mathbf{X}}_{TT} \simeq 1.24 \times 10^{-16} \text{ m/s}^2$ for a MEO orbiter. In addition, $\ddot{U}_{\text{ext}} = d^2 U_{\text{ext}} / dTT^2 + \mathcal{O}(c^{-2})$ has the form

$$\begin{aligned} \ddot{U}_{\text{ext}} \equiv \frac{d^2 U_{\text{ext}}}{dTT^2} &= - \sum_{B \neq E} \frac{GM_B}{r_{BE}^3} \left((\mathbf{a}_B - \mathbf{a}_E) \cdot (\mathbf{x}_B - \mathbf{x}_E) + \right. \\ &+ \left. (\mathbf{v}_B - \mathbf{v}_E) \cdot (\mathbf{v}_B - \mathbf{v}_E) - \frac{3}{r_{BE}^2} \left((\mathbf{v}_B - \mathbf{v}_E) \cdot (\mathbf{x}_B - \mathbf{x}_E) \right)^2 \right) + \mathcal{O}(c^{-2}), \quad (32) \end{aligned}$$

with GM_B , \mathbf{r}_B and \mathbf{v}_B being the mass parameter and barycentric position and velocity vectors of body B, E is the index for Earth and r_{BE} is the geocentric range of body B and $r_{BE} = |\mathbf{x}_E - \mathbf{x}_B|$.

2. Transforming velocity and acceleration

Now, we can present the expressions that describe the velocity and acceleration transformations. To do this, starting with the velocity, we use (22), (24), (26), and (29), which yield

$$\begin{aligned} (\dot{\mathbf{x}} - \dot{\mathbf{x}}_E)_{\text{TDB}} &= \dot{\mathbf{X}}_{TT} + c^{-2} \left\{ \left(\frac{1}{2} v_E^2 + (1 + \gamma) U_{\text{ext}} + 2(\mathbf{a}_E \cdot \mathbf{X}) + (\mathbf{v}_E \cdot \dot{\mathbf{X}}) \right) \dot{\mathbf{X}} + \frac{1}{2} \left((\mathbf{a}_E \cdot \mathbf{X}) + (\mathbf{v}_E \cdot \dot{\mathbf{X}}) \right) \mathbf{v}_E + \right. \\ &+ \left. \left(\frac{1}{2} (\mathbf{v}_E \cdot \mathbf{X}) - (\mathbf{X} \cdot \dot{\mathbf{X}}) \right) \mathbf{a}_E + \left((\dot{\mathbf{a}}_E \cdot \mathbf{X}) + (\mathbf{a}_E \cdot \dot{\mathbf{X}}) + \gamma \dot{U}_{\text{ext}} \right) \mathbf{X} - \frac{1}{2} X^2 \dot{\mathbf{a}}_E \right\}_{TT} + \mathcal{O} \left(8.49 \times 10^{-13} \text{ m/s} \right). \quad (33) \end{aligned}$$

Note that all the quantities on the right-hand side of (33) are TT-compatible.

Similarly, we have the expression for transforming the acceleration between the two reference systems. For this, we will use (22), (25), (27)–(28), and (31), which yield the following:

$$\begin{aligned} (\ddot{\mathbf{x}} - \ddot{\mathbf{x}}_E)_{\text{TDB}} &= \ddot{\mathbf{X}}_{TT} + L_C \ddot{\mathbf{X}}_{TT} + c^{-2} \left\{ \left(v_E^2 + (2 + \gamma) U_{\text{ext}} + 3(\mathbf{a}_E \cdot \mathbf{X}) + 2(\mathbf{v}_E \cdot \dot{\mathbf{X}}) \right) \ddot{\mathbf{X}} + \right. \\ &+ \left((\mathbf{v}_E \cdot \mathbf{a}_E) + (1 + 2\gamma) \dot{U}_{\text{ext}} + 3(\dot{\mathbf{a}}_E \cdot \mathbf{X}) + 4(\mathbf{a}_E \cdot \dot{\mathbf{X}}) + (\mathbf{v}_E \cdot \ddot{\mathbf{X}}) \right) \dot{\mathbf{X}} + \\ &+ \frac{1}{2} \left((\dot{\mathbf{a}}_E \cdot \mathbf{X}) + 2(\mathbf{a}_E \cdot \dot{\mathbf{X}}) + (\mathbf{v}_E \cdot \ddot{\mathbf{X}}) \right) \mathbf{v}_E + \left((\mathbf{a}_E \cdot \mathbf{X}) + (\mathbf{v}_E \cdot \dot{\mathbf{X}}) - (\dot{\mathbf{X}} \cdot \dot{\mathbf{X}}) - (\mathbf{X} \cdot \ddot{\mathbf{X}}) \right) \mathbf{a}_E + \\ &+ \left(\frac{1}{2} (\mathbf{v}_E \cdot \mathbf{X}) - 2(\mathbf{X} \cdot \dot{\mathbf{X}}) \right) \dot{\mathbf{a}}_E + \left(\gamma \ddot{U}_{\text{ext}} + (\ddot{\mathbf{a}}_E \cdot \mathbf{X}) + 2(\dot{\mathbf{a}}_E \cdot \dot{\mathbf{X}}) + (\mathbf{a}_E \cdot \ddot{\mathbf{X}}) \right) \mathbf{X} - \frac{1}{2} X^2 \ddot{\mathbf{a}}_E \Big\}_{TT} + \\ &+ \mathcal{O} \left(1.24 \times 10^{-16} \text{ m/s}^2 \right), \quad (34) \end{aligned}$$

where the error terms in these expressions are set by the omitted L_C^2 terms.

The screening and remainder bounds in this section are computed using the parameter envelopes in Table II, representative of (i) a terrestrial station and (ii) a GNSS MEO spacecraft. For other regimes (e.g., GEO, HEO, lunar transfer, NRHO), the retained terms should be re-screened using the same procedure with updated envelopes for $(\mathbf{X}, \dot{\mathbf{X}}, \ddot{\mathbf{X}})$ and the relevant external potentials and accelerations.

D. Practical form for the relevant expressions

Results (17)–(18), (33), and (34) have many terms that may be too small. We estimate the magnitudes of the terms in these expressions using Table II, which provides the nominal values for the quantities involved. This will help us

TABLE II. Approximate values for various parameters involved.

Notation	Meaning	Value
γ	Parametrized post-Newtonian (PPN) parameter	1
GM_S	Solar gravitational constant	$1.32712442099 \times 10^{20} \text{ m}^3 \text{ s}^{-2}$
r_E	Earth's position relative to barycenter	1 AU = 149 597 870 700.0 m
\mathbf{v}_E	Earth's velocity relative to barycenter	$29.78 \times 10^3 \text{ m/s}$
<i>Ground-based station:</i>		
\mathbf{X}_S	position relative to the center of the Earth	$6378.1 \times 10^3 \text{ m}$
$\dot{\mathbf{X}}_S$	velocity relative to the center of the Earth	$(2\pi/\text{day})R_E = 463.83 \text{ m/s}$
$\ddot{\mathbf{X}}_S$	acceleration relative to the center of the Earth	$(2\pi/\text{day})^2 R_E = 3.37 \times 10^{-2} \text{ m/s}^2$
<i>MEO spacecraft at altitude of $h = 20200 \text{ km}$</i>		
\mathbf{X}_{MEO}	position relative to the center of the Earth	$26578.1 \times 10^3 \text{ m}$
$\dot{\mathbf{X}}_{\text{MEO}}$	velocity relative to the center of the Earth	$3.87 \times 10^3 \text{ m/s}$
$\ddot{\mathbf{X}}_{\text{MEO}}$	acceleration relative to the center of the Earth	0.56 m/s^2

understand the changes in station or satellite coordinates relative to the Earth's center of mass in the barycentric frame. We also recognize that the solar gravitational potential provides the largest contribution to U_{ext} .

Numerically at the geocenter, $GM_S/\text{AU} \simeq 8.87 \times 10^8 \text{ m}^2/\text{s}^2$ while $GM_M/r_{\text{EM}} \simeq 1.28 \times 10^4 \text{ m}^2/\text{s}^2$, so the solar term dominates U_{ext} by $\sim 7 \times 10^4$ (the remaining planetary terms are smaller still for Earth-orbiting applications).

As the characteristic magnitudes of ($|\mathbf{X}|, |\dot{\mathbf{X}}|, |\ddot{\mathbf{X}}|$) for a MEO (GPS-like) spacecraft exceed those of a ground-based station (Table II), we screen the transformation terms using the MEO envelope to obtain conservative bounds. We consider the transformations for a MEO orbiter (i.e., a GPS spacecraft), with the position, velocity and the acceleration present in (17)–(18), (33), and (34) take the relevant values of MEO orbiter (i.e., a GPS spacecraft), namely $(\mathbf{X}, \dot{\mathbf{X}}, \ddot{\mathbf{X}}) \rightarrow (\mathbf{X}_{\text{MEO}}, \dot{\mathbf{X}}_{\text{MEO}}, \ddot{\mathbf{X}}_{\text{MEO}})$, that are given in Table II. With these values, we use (18) to estimate contribution of the various terms in the position transformation:

$$\left(L_C + c^{-2}\gamma U_{\text{ext}}\right)\mathbf{X} \approx 0.66 \text{ m}, \quad c^{-2}\left\{\frac{1}{2}(\mathbf{v}_E \cdot \mathbf{X})\mathbf{v}_E\right\} \approx 0.13 \text{ m}, \quad c^{-2}\left\{(\mathbf{a}_E \cdot \mathbf{X})\mathbf{X} - \frac{1}{2}X^2\mathbf{a}_E\right\} \lesssim 7.00 \times 10^{-5} \text{ m}. \quad (35)$$

Note that the acceleration-dependent terms in (35) are very small and are currently considered practically irrelevant. Consequently, a reasonable approximation of (17)–(18) for a MEO orbiter would be, as outlined in [1],

$$(\mathbf{x} - \mathbf{x}_E)_{\text{TDB}} = \mathbf{X}_{\text{TT}} - L_C\mathbf{X}_{\text{TT}} - c^{-2}\left\{\frac{1}{2}(\mathbf{v}_E \cdot \mathbf{X})\mathbf{v}_E + \gamma U_{\text{ext}}\mathbf{X}\right\}_{\text{TT}} + \mathcal{O}\left(7.01 \times 10^{-5} \text{ m}\right), \quad (36)$$

where the error bound is provided by the omitted acceleration-dependent terms shown in (35). Note that the same expression is valid for a ground-based station with the error term being of the order of $\mathcal{O}(4.03 \times 10^{-6} \text{ m})$.

Eq. (36) is closely related to the station-coordinate transformations used in DSN radiometric modeling (e.g., range and Doppler) [1]. Relative to commonly used operational forms, we keep the explicit scale term L_C and track the small acceleration-dependent contributions and their remainder bound, which become relevant when demanding mm-level frame-closure consistency and 10^{-16} -level time/frequency transfer budgets. For GNSS cm-class processing the additional screened terms provide a conservative, implementation-ready state map between TT-compatible GCRS and TDB-compatible BCRS.

Next, we evaluate the terms present in the velocity transformation in (33) as below

$$c^{-2}\left\{\left(\frac{1}{2}v_E^2 + (1 + \gamma)U_{\text{ext}}\right)\dot{\mathbf{X}}\right\} \approx 9.56 \times 10^{-5} \text{ m/s}, \quad c^{-2}\left\{(\mathbf{v}_E \cdot \dot{\mathbf{X}})\dot{\mathbf{X}}\right\} \approx 4.96 \times 10^{-6} \text{ m/s}, \quad (37)$$

$$c^{-2}\left\{2(\mathbf{a}_E \cdot \mathbf{X})\dot{\mathbf{X}}\right\} \approx 1.36 \times 10^{-8} \text{ m/s}, \quad c^{-2}\left\{\frac{1}{2}(\mathbf{v}_E \cdot \dot{\mathbf{X}})\mathbf{v}_E\right\} \approx 3.82 \times 10^{-5} \text{ m/s} \quad (38)$$

$$c^{-2}\left\{\frac{1}{2}(\mathbf{a}_E \cdot \mathbf{X})\mathbf{v}_E\right\} \approx 2.61 \times 10^{-8} \text{ m/s}, \quad c^{-2}\left\{(\mathbf{X} \cdot \dot{\mathbf{X}})\mathbf{a}_E\right\} \lesssim 3.40 \times 10^{-9} \text{ m/s}, \quad (39)$$

$$c^{-2}\left\{\frac{1}{2}(\mathbf{v}_E \cdot \mathbf{X})\mathbf{a}_E\right\} \approx 2.61 \times 10^{-8} \text{ m/s}, \quad c^{-2}\left\{\gamma\dot{U}_{\text{ext}}\mathbf{X}\right\} \approx 5.22 \times 10^{-8} \text{ m/s}, \quad (40)$$

$$c^{-2}\left\{\left((\dot{\mathbf{a}}_E \cdot \mathbf{X}) + (\mathbf{a}_E \cdot \dot{\mathbf{X}})\right)\mathbf{X}\right\} \approx 6.81 \times 10^{-9} \text{ m/s}, \quad c^{-2}\left\{\frac{1}{2}X^2\dot{\mathbf{a}}_E\right\} \approx 9.28 \times 10^{-12} \text{ m/s}. \quad (41)$$

As a result, limiting the terms at $4.96 \times 10^{-6} \text{ m/s}$, from (33), we have the following for the velocity transformation:

$$(\dot{\mathbf{x}} - \dot{\mathbf{x}}_E)_{\text{TDB}} = \dot{\mathbf{X}}_{\text{TT}} - c^{-2}\left\{\left(\frac{1}{2}v_E^2 + (1 + \gamma)U_{\text{ext}} + (\mathbf{v}_E \cdot \dot{\mathbf{X}})\right)\dot{\mathbf{X}} + \frac{1}{2}(\mathbf{v}_E \cdot \dot{\mathbf{X}})\mathbf{v}_E\right\}_{\text{TT}} + \mathcal{O}\left(1.29 \times 10^{-7} \text{ m/s}\right), \quad (42)$$

TABLE III. Screened operational transformations and conservative remainder bounds using the envelopes in Table II.

Transformation	Position	Velocity	Acceleration
Screened form (TT→TDB)	Eq. (36)	Eq. (42)	Eq. (51)
Remainder bound (ground)	4.03×10^{-6} m	9.73×10^{-8} m/s	5.27×10^{-15} m/s ²
Remainder bound (MEO)	7.01×10^{-5} m	1.29×10^{-7} m/s	6.68×10^{-14} m/s ²

where the error bound results from the omitted acceleration-dependent and \dot{U}_{ext} terms. It is worth noting that result (42) includes two additional terms compared to [1]. The same expression is also applicable to ground-based stations, with the corresponding error term being on the order of $\mathcal{O}(9.73 \times 10^{-8}$ m/s).

Finally, we evaluate the terms involved in the acceleration transformations (34) as below

$$L_c \ddot{\mathbf{X}} \approx 8.36 \times 10^{-9} \text{ m/s}^2, \quad c^{-2} \left\{ \frac{1}{2} \left(2(\mathbf{a}_E \cdot \dot{\mathbf{X}}) + (\mathbf{v}_E \cdot \ddot{\mathbf{X}}) \right) \mathbf{v}_E \right\} \approx 2.97 \times 10^{-9} \text{ m/s}^2, \quad (43)$$

$$c^{-2} \left\{ \left(v_E^2 + (2 + \gamma) U_{\text{ext}} + 3(\mathbf{a}_E \cdot \mathbf{X}) + 2(\mathbf{v}_E \cdot \dot{\mathbf{X}}) \right) \ddot{\mathbf{X}} \right\} \approx 2.37 \times 10^{-8} \text{ m/s}^2, \quad (44)$$

$$c^{-2} \left\{ \left((\mathbf{v}_E \cdot \mathbf{a}_E) + (1 + 2\gamma) \dot{U}_{\text{ext}} + 4(\mathbf{a}_E \cdot \dot{\mathbf{X}}) + (\mathbf{v}_E \cdot \ddot{\mathbf{X}}) \right) \dot{\mathbf{X}} \right\} \approx 7.58 \times 10^{-10} \text{ m/s}^2, \quad (45)$$

$$c^{-2} \left\{ 3(\dot{\mathbf{a}}_E \cdot \mathbf{X}) \dot{\mathbf{X}} \right\} \approx 8.11 \times 10^{-15} \text{ m/s}^2, \quad c^{-2} \left\{ \frac{1}{2} (\dot{\mathbf{a}}_E \cdot \mathbf{X}) \mathbf{v}_E \right\} \approx 1.40 \times 10^{-14} \text{ m/s}^2, \quad (46)$$

$$c^{-2} \left\{ \left((\mathbf{a}_E \cdot \mathbf{X}) + (\mathbf{v}_E \cdot \dot{\mathbf{X}}) - (\dot{\mathbf{X}} \cdot \dot{\mathbf{X}}) - (\mathbf{X} \cdot \ddot{\mathbf{X}}) \right) \mathbf{a}_E \right\} \approx 9.60 \times 10^{-12} \text{ m/s}^2, \quad (47)$$

$$c^{-2} \left\{ \left(\frac{1}{2} (\mathbf{v}_E \cdot \mathbf{X}) - 2(\mathbf{X} \cdot \dot{\mathbf{X}}) \right) \dot{\mathbf{a}}_E \right\} \approx 1.58 \times 10^{-14} \text{ m/s}^2, \quad (48)$$

$$c^{-2} \left\{ \left(\gamma \ddot{U}_{\text{ext}} + (\ddot{\mathbf{a}}_E \cdot \mathbf{X}) + 2(\dot{\mathbf{a}}_E \cdot \dot{\mathbf{X}}) \right) \mathbf{X} \right\} \approx 3.70 \times 10^{-14} \text{ m/s}^2, \quad (49)$$

$$c^{-2} \left\{ (\mathbf{a}_E \cdot \ddot{\mathbf{X}}) \mathbf{X} \right\} \approx 9.90 \times 10^{-13} \text{ m/s}^2, \quad c^{-2} \left\{ \frac{1}{2} X^2 \ddot{\mathbf{a}}_E \right\} \approx 7.35 \times 10^{-18} \text{ m/s}^2. \quad (50)$$

As a result, limiting the terms to $\mathcal{O}(1 \times 10^{-13}$ m/s²), we have the following expression to transform acceleration:

$$\begin{aligned} (\ddot{\mathbf{x}} - \ddot{\mathbf{x}}_E)_{\text{TDB}} &= \ddot{\mathbf{X}}_{\text{TT}} + L_c \ddot{\mathbf{X}}_{\text{TT}} - c^{-2} \left\{ \left(v_E^2 + (2 + \gamma) U_{\text{ext}} + 3(\mathbf{a}_E \cdot \mathbf{X}) + 2(\mathbf{v}_E \cdot \dot{\mathbf{X}}) \right) \ddot{\mathbf{X}} + \right. \\ &+ \left((\mathbf{v}_E \cdot \mathbf{a}_E) + (1 + 2\gamma) \dot{U}_{\text{ext}} + 4(\mathbf{a}_E \cdot \dot{\mathbf{X}}) + (\mathbf{v}_E \cdot \ddot{\mathbf{X}}) \right) \dot{\mathbf{X}} + \left((\mathbf{a}_E \cdot \dot{\mathbf{X}}) + \frac{1}{2} (\mathbf{v}_E \cdot \ddot{\mathbf{X}}) \right) \mathbf{v}_E + \\ &+ \left. \left((\mathbf{a}_E \cdot \mathbf{X}) + (\mathbf{v}_E \cdot \dot{\mathbf{X}}) - (\dot{\mathbf{X}} \cdot \dot{\mathbf{X}}) - (\mathbf{X} \cdot \ddot{\mathbf{X}}) \right) \mathbf{a}_E + (\mathbf{a}_E \cdot \ddot{\mathbf{X}}) \mathbf{X} \right\}_{\text{TT}} + \mathcal{O}\left(6.68 \times 10^{-14} \text{ m/s}^2\right), \quad (51) \end{aligned}$$

where the error bound is from the group of the omitted terms involving $\dot{\mathbf{a}}_E$ and \ddot{U}_{ext} derivatives. It is worth noting that result (51) includes several additional terms compared to [1]. Also, the same expression is also applicable to ground-based stations, with the corresponding error term being on the order of $\mathcal{O}(5.27 \times 10^{-15}$ m/s²).

Therefore, considering realistic measurement accuracies, we refer to the magnitudes of various terms conducted for a MEO orbiter. Consequently, the expressions (36), (42), and (51) are recommended for position, velocity, and acceleration transformations when GNSS data processing is concerned. These results represent the set of the expressions recommended to transform position, velocity and acceleration vectors as needed to process GNSS data from either GCRS or BCRS. These formulae are accurate to order c^{-2} and the corrective terms can be evaluated using for \mathbf{X}_{TT} , \mathbf{V}_{TT} and \mathbf{A}_{TT} in TT-compatible GCRS or TDB-compatible BCRS quantities translated to the geocenter. These formulae are accurate to $\mathcal{O}(c^{-2})$. We adopt GR (i.e., $\gamma = 1$) for all numerical results.

We note that expressions in [1] are derived in the context of DSN radiometric observables (two-way range, Doppler, and ΔDOR) and is typically used in models where station acceleration terms are negligible at the required accuracy. In contrast, GNSS processing uses one-way code and carrier-phase observables, and our goal here is dynamical consistency of the full state mapping (position–velocity–acceleration) at the millimeter level; therefore we retain the acceleration-dependent terms that are dropped in the traditional DSN form.

Recommended transformations: For cm/ps-class GNSS, use Eq. (36) for position with the two leading c^{-2} terms (scale and Lorentz), Eq. (42) for velocity with the three leading c^{-2} terms, and Eq. (51) for acceleration retaining terms $\gtrsim 10^{-13}$ m/s². These screened sets were used in the 24 h end-to-end frame-closure test of Fig. 1; the bounds below quantify the truncation error introduced solely by screening of the closed-form transformations.

The inverse transformations to (36), (42), and (51) are obtained by interchanging $(\mathbf{r}_E)_{\text{TDB}} = (\mathbf{x} - \mathbf{x}_E)_{\text{TDB}}$ with \mathbf{X}_{TT} , $(\dot{\mathbf{r}}_E)_{\text{TDB}} = (\dot{\mathbf{x}} - \dot{\mathbf{x}}_E)_{\text{TDB}} = (\mathbf{v} - \mathbf{v}_E)_{\text{TDB}}$ with \mathbf{V}_{TT} , and $(\ddot{\mathbf{r}}_E)_{\text{TDB}} = (\ddot{\mathbf{x}} - \ddot{\mathbf{x}}_E)_{\text{TDB}} = (\mathbf{a} - \mathbf{a}_E)_{\text{TDB}}$ with \mathbf{A}_{TT} in all 3 equations and inverting the sign of all corrective terms, as evident from (13) and (15).

For 24 h spans with cm/ps-class observables, enforce

$$\sup_t \|\delta \mathbf{r}\| \leq 7.01 \times 10^{-5} \text{ m}, \quad \sup_t \|\delta \mathbf{v}\| \leq 1.29 \times 10^{-7} \text{ m s}^{-1}, \quad \sup_t \|\delta \mathbf{a}\| \leq 6.68 \times 10^{-14} \text{ m s}^{-2},$$

matching the remainders from Eqs. (36), (42), and (51) used in our closures. Here $\|\cdot\|$ denotes the Euclidean norm, and $\delta \mathbf{r}(t), \delta \mathbf{v}(t), \delta \mathbf{a}(t)$ are the sums of the omitted terms in the screened position, velocity, and acceleration transformations, respectively. These conservative limits are intended as regression thresholds for the transformations themselves; the end-to-end closure residuals of Sec. III additionally include numerical-integration and force-model consistency errors. For $\Delta T = 24$ h, these bounds correspond to worst-case state impacts of $\delta r \sim 7 \times 10^{-5}$ m directly from the position remainder, $\delta r \sim (\delta v)\Delta T \approx 1.1$ cm from the velocity remainder, and $\delta r \sim \frac{1}{2}(\delta a)\Delta T^2 \approx 2.5 \times 10^{-4}$ m (0.25 mm) from the acceleration remainder. Thus the screened acceleration set is consistent with the millimeter-level closure target, while the screened velocity set remains within a centimeter-class envelope over one day.

Finally, mass parameters of celestial bodies, GM , must also be transformed between their value in the TT-compatible GCRS, $(GM)_{\text{TT}}$, and the TDB-compatible value in BCRS, $(GM)_{\text{TDB}}$, as:

$$(GM)_{\text{TDB}} = (1 - L_C)(GM)_{\text{TT}}, \quad (52)$$

which may be obtained from (8) and (11), by equating $(GM)_{\text{TCB}} = (GM)_{\text{TCG}}$ and using (10).

We stress that dynamical parameters tied to a TDB-compatible ephemeris (e.g., DE440) *must not* be re-scaled when used with Eqs. (51)–(52); only the *labels* of the time arguments change. The IAU constants used are $L_C = 6.969290134 \times 10^{-10}$ and $L_B = 1.550519768 \times 10^{-8}$, with the conventional $\text{TDB}_0 \simeq -65.5 \mu\text{s}$.

Implementation note (GM scaling & ephemeris argument): This work adopts TDB as the ephemeris argument. For JPL DE430/DE440-family kernels [33], the delivered (GM) values are already TDB-consistent; use Eq. (52) only when converting a TT-referenced constant, i.e., $(GM)_{\text{TDB}} = (1 - L_C)(GM)_{\text{TT}}$ and inversely $(GM)_{\text{TT}} = (1 - L_C)^{-1}(GM)_{\text{TDB}}$. Do not rescale any (GM) that is tied to a TDB-based kernel.

E. Minimal cislunar regression test: NRHO-like geometry

We give a compact, implementation-ready regression test that exercises the Earth (GCRS/BCRS) and Moon (LCRS) transformation chain and the 1PN barycentric light-time model. Here “NRHO” denotes a near-rectilinear halo orbit about the Earth–Moon L_2 region. The test geometry consists of (i) an Earth-based tracking station with TT-compatible coordinates (ITRF→GCRS), and (ii) a cislunar user spacecraft in an NRHO-like orbit about the Moon, whose state is propagated in the TDB-compatible BCRS and mapped to the LCRS using Appendix A [Eqs. (A25)–(A27)]. This is a regression/consistency test of the relativistic reference-system infrastructure; end-to-end cislunar GNSS user positioning performance additionally depends on signal availability and estimation strategy [34, 35]. Specifically,

Order-of-magnitude check: For an NRHO-like envelope $|\mathbf{X}| \sim 10^8$ m and $|\mathbf{v}_M| \sim 1$ km/s, the LCRS time-coupling term $c^{-2}(\mathbf{v}_M \cdot \mathbf{X})$ is at the $\sim 10^{-6}$ s level, while the leading spatial correction $\sim c^{-2}v_M^2 \mathbf{X}$ is at the $\sim 10^{-3}$ m level. These scales motivate retaining the full $\mathcal{O}(c^{-2})$ LCRS terms for cm-level light-time and state modeling in Earth–Moon geometries.

State propagation and transformations: Propagate the spacecraft state in the BCRS with the same dynamical model used for the MEO test (relativistic point-mass terms and geopotential terms exactly as in the main text), and adopt the screened operational forms for position, velocity, and acceleration, Eqs. (36), (42), and (51), respectively. Map spacecraft and ground states to the LCRS using Eqs. (A25) and (A26) for position and velocity; accelerations follow the same screening logic as in the Earth case (see Table IV for configuration details).

Observables and light-time: Compute one-way light-time between a ground station and the cislunar spacecraft with (64). Retain Sun and Earth Shapiro terms only; other bodies are negligible at the accuracy targeted here. (Note that most of the solar term behaves as a range scale and cancels in differenced observables, but keep it for absolute light-time consistency at the centimeter level over ΔT .) Use the same TT/TDB handling and GM scaling guidance as in Sec. IID to avoid double-scaling when using TDB-consistent ephemerides. The lunar Shapiro delay is negligible at the accuracy targeted here: a rough upper bound is $\Delta t_{\text{Shapiro}}^{\text{Moon}} \sim 2GM_M c^{-3} \ln(\dots) \lesssim \mathcal{O}(1 \text{ ps})$, corresponding to $\lesssim 0.3$ mm in range, i.e., well below the cm-class absolute light-time envelope adopted in this test.

Closure metric (BCRS→LCRS→BCRS): Define the cislunar frame-closure for position and velocity over an analysis span ΔT as

$$\Delta \mathbf{r}(t) \equiv \mathbf{r}_{\text{BCRS} \rightarrow \text{LCRS} \rightarrow \text{BCRS}}(t) - \mathbf{r}_{\text{BCRS}}(t), \quad \Delta \mathbf{v}(t) \equiv \mathbf{v}_{\text{BCRS} \rightarrow \text{LCRS} \rightarrow \text{BCRS}}(t) - \mathbf{v}_{\text{BCRS}}(t), \quad (53)$$

and require that the sup norms over $t \in [t_0, t_0 + \Delta T]$ do not exceed the screening remainders already specified under Eqs. (36) and (42), respectively. In this regression test we adopt the same truncation budgets as for the Earth MEO screening (Table III) to bound the error introduced solely by the screened state transformations. This ensures that

TABLE IV. Configuration for the cislunar check in Sec. II E (NRHO-like geometry, Earth relay).

Ephemerides and time scales	DE440 (TDB); TT/TDB transformations as in Eqs. (12)–(15)
State propagation frame	BCRS
Dynamics (spacecraft)	Same relativistic and geopotential model as used for MEO closure
Operational transformations (Earth)	Position/velocity/accel: Eqs. (36), (42), (51)
LCRS transformations (Moon)	Position/velocity (A25), (A26); acceleration (A27).
Light-time and delays	Eq. (64); Shapiro bodies: Sun, Earth
Closure metric	Eq. (53); thresholds tied to remainders of Eqs. (36), (42)
Span ΔT	24 h (nominal); longer spans permissible for operational testing

all omitted terms remain below the stated operational error budgets for the specific state and geometry envelope used to size the screened remainder bounds; for mission-specific cislunar operations, the same remainder analysis should be re-evaluated with an NRHO-appropriate envelope for $(|\mathbf{X}|, |\dot{\mathbf{X}}|, |\ddot{\mathbf{X}}|)$.

As an order-of-magnitude check for Earth–Moon geometries, consider a representative NRHO with $|\mathcal{X}| \sim 7 \times 10^7$ m in the LCRS and the Moon’s barycentric speed $|\mathbf{v}_M| \sim 10^3$ m/s. The leading $\mathcal{O}(c^{-2})$ time term in the BCRS \leftrightarrow LCRS map scales as $(\mathbf{v}_M \cdot \mathcal{X})/c^2 \sim 0.8 \mu\text{s}$, while the associated Lorentz-type spatial correction scales as $(v_M^2/c^2)|\mathcal{X}| \sim 10^{-3}$ m (sub-mm). For an Earth–Moon light path, the Earth Shapiro delay is typically $\mathcal{O}(10-10^2)$ ps (cm range-equivalent), whereas the Moon Shapiro delay is bounded by $(1 + \gamma)GM_M c^{-3} \ln(\dots) \lesssim \mathcal{O}(1)$ ps (< 1 mm) and is neglected here consistently with the cm-class absolute light-time envelope adopted in this regression test.

Practical notes: (i) Use the same station coordinates and Earth-orientation handling as in the MEO test so that any differences trace solely to the frame transformations. (ii) When constructing differenced observables, the solar Shapiro contribution behaves dominantly as a scale; retain it for absolute range, document its cancellation otherwise. (iii) Publish the reference states and resulting $\Delta \mathbf{r}, \Delta \mathbf{v}$ statistics for this case alongside those of the MEO closure to enable external regression tests.

F. Transformation between the proper time and TDB in BCRS

1. Direct transformations: TDB \rightarrow proper time

Considering GNSS applications in cislunar environment we may use a truncated version of the metric tensor of the BCRS (see details in [21]). Then, to sufficient accuracy, the transformation between the proper time of an observer τ and the coordinate time in the BCRS, TCB, is given as below:

$$\frac{d\tau}{dT_{\text{TCB}}} = 1 - \frac{1}{c^2} \left\{ \frac{1}{2} v_0^2 + \sum_{\text{B}} \frac{GM_{\text{B}}}{r_{\text{B}0}} \left(1 - J_{\text{B}2} \left(\frac{R_{\text{B}}}{r_{\text{B}0}} \right)^2 P_{20}(\cos \theta_{\text{B}}) \right) \right\}_{\text{TCB}} + \mathcal{O}(8.77 \times 10^{-17}), \quad (54)$$

where $\mathbf{x}_0, \mathbf{v}_0 = \dot{\mathbf{x}}_0$, and $v_0 = |\mathbf{v}_0|$ represent the BCRS position and velocity vectors of the spacecraft; $\mathbf{r}_{\text{B}0} = \mathbf{x}_{\text{B}} - \mathbf{x}_0$ is the separation vector between a body B and the spacecraft, $r_{\text{B}0} = |\mathbf{r}_{\text{B}0}|$; also we define $\cos \theta_{\text{B}} = (\mathbf{n}_{\text{B}0} \cdot \mathbf{s}_{\text{B}})$, where \mathbf{s}_{B} is the unit vector along the axis of rotation for the body B .

Note that we retained only the quadrupole ($J_{2,\text{B}}$) contribution in the multipolar correction. Higher harmonics scale as $J_{\ell,\text{B}}(R_{\text{B}}/r_{\text{B}0})^\ell$ and are therefore suppressed by at least $(R_{\text{B}}/r_{\text{B}0})^2$ relative to the $J_{2,\text{B}}$ term. For the Earth at a GPS altitude, $(R_{\text{E}}/r)^2 \simeq 0.058$ and $|J_{4,\text{E}}/J_{2,\text{E}}| \sim 10^{-3}$, implying a fractional size $\lesssim 10^{-4}$ of the J_2 correction, i.e., $\lesssim 10^{-18}$ in $d\tau/dt$, below the 5×10^{-18} metric cutoff used in Sec. III B 1. See, e.g., Refs. [5, 7] for conventions and typical harmonic magnitudes. Ultimately, the error bound in (54) came from the omitted contribution of the $1/c^4$ -terms (see [21]), that for a GPS spacecraft evaluated to have magnitude of $c^{-4} \left(-\frac{1}{8} v_0^4 - \frac{3}{2} v_0^2 w_0 + 4(\mathbf{v}_0 \cdot \mathbf{w}) + \frac{1}{2} w_0^2 + \Delta \right) \simeq 8.77 \times 10^{-17}$. As a result, we may neglect these terms for GNSS applications in cislunar environment.

Taking into account (11), the relationships between the TDB- and TCB-compatible quantities yield a relation for the rates of an observer’s proper time and TDB. Specifically, by applying (11) and using the chain rule for derivatives, $d\tau/dT_{\text{DB}} = (d\tau/dT_{\text{CB}})(dT_{\text{CB}}/dT_{\text{DB}}) = (d\tau/dT_{\text{CB}})/(1 - L_{\text{B}})$, we obtain the following result:

$$\frac{d\tau}{dT_{\text{DB}}} = \frac{1}{1 - L_{\text{B}}} \left(1 - \frac{1}{c^2} \left\{ \frac{1}{2} v_0^2 + \sum_{\text{B}} \frac{GM_{\text{B}}}{r_{\text{B}0}} \left(1 - \frac{J_{\text{B}2} R_{\text{B}}^2}{2r_{\text{B}0}^2} (3(\mathbf{n}_{\text{B}0} \cdot \mathbf{s}_{\text{B}})^2 - 1) \right) \right\}_{\text{TDB}} \right) + \mathcal{O}(8.77 \times 10^{-17}). \quad (55)$$

Integrating (55) provides an expression that relates the interval of the elapsed proper time τ during a particular

interval of TDB $\in [\text{TDB}, \text{TDB}_\tau]$:

$$\begin{aligned} \tau = & \frac{1}{1 - L_B} \left(\text{TDB} - \text{TDB}_\tau - \frac{1}{c^2} \int_{\text{TDB}_\tau}^{\text{TDB}} \left\{ \frac{1}{2} v_0^2 + \sum_B \frac{GM_B}{r_{B0}} \left(1 - \frac{J_{B2} R_B^2}{2r_{B0}^2} (3(\mathbf{n}_{B0} \cdot \mathbf{s}_B)^2 - 1) \right) \right\}_{\text{TDB}} dt \right) + \\ & + \mathcal{O}(8.77 \times 10^{-17})(\text{TDB} - \text{TDB}_\tau), \end{aligned} \quad (56)$$

where \mathbf{r}_0 and $\mathbf{v}_0 = d\mathbf{r}_0/dt$ are the barycentric position and velocity of the spacecraft, $\mathbf{r}_{B0} = \mathbf{r}_B - \mathbf{r}_0$ is the separation vector from the spacecraft to body B , with $\mathbf{n}_{B0} = \mathbf{r}_{B0}/r_{B0}$ being the corresponding unit vector, and \mathbf{s}_B is the unit vector along the axis of the rotation, TDB_τ is the beginning of the integration interval.

2. Inverse transformations: proper time \rightarrow TDB

Similarly to (54), we determine the inverse transformation from the proper time to the TCB:

$$\frac{d\text{TCB}}{d\tau} = 1 + \frac{1}{c^2} \left\{ \frac{1}{2} v_0^2 + \sum_B \frac{GM_B}{r_{B0}} \left(1 - J_{B2} \left(\frac{R_B}{r_{B0}} \right)^2 P_{20}(\cos \theta_B) \right) \right\}_\tau + \mathcal{O}(1.37 \times 10^{-16}), \quad (57)$$

where then error bound came from the omitted contribution of the c^{-4} -terms in the inverse transformation that were estimated to contribute effect on the order of $c^{-4} \left(\frac{3}{8} v^4 + \frac{5}{2} v^2 w_0 - 4(\mathbf{v} \cdot \mathbf{w}) + \frac{1}{2} w_0^2 - \Delta \right) \simeq 1.37 \times 10^{-16}$. As such, these terms are too small to account for GNSS applications in cislunar space, thus, they may be neglected.

Taking into account the relationship between TCB and TDB, given by (11), we develop an expression relating the rates of TDB and observer's proper time, which from $d\text{TDB}/d\tau = (d\text{TDB}/d\text{TCB}) d\text{TCB}/d\tau = (1 - L_B) d\text{TCB}/d\tau$, results in:

$$\frac{d\text{TDB}}{d\tau} = (1 - L_B) \left(1 + \frac{1}{c^2} \left\{ \frac{1}{2} v_0^2 + \sum_B \frac{GM_B}{r_{B0}} \left(1 - J_{B2} \left(\frac{R_B}{r_{B0}} \right)^2 P_{20}(\cos \theta_B) \right) \right\}_\tau \right) + \mathcal{O}(1.37 \times 10^{-16}). \quad (58)$$

Integrating (58) over τ from τ_0 to τ provides a relation between the proper time and TDB:

$$\text{TDB} = (1 - L_B) \left(\Delta\tau + \frac{1}{c^2} \int_{\tau_0}^{\tau} \left\{ \frac{1}{2} v_0^2 + \sum_B \frac{GM_B}{r_{B0}} \left(1 - J_{B2} \left(\frac{R_B}{r_{B0}} \right)^2 P_{20}(\cos \theta_B) \right) \right\}_\tau dt \right) + \mathcal{O}(1.37 \times 10^{-16}) \Delta\tau, \quad (59)$$

where the relativistic time equation at the clock is given as

$$\tau = t^* - \frac{1}{c^2} \int_{t_0}^{t^*} \left\{ \frac{1}{2} v_0^2 + \sum_B \frac{GM_B}{r_{B0}} \left(1 - J_{B2} \left(\frac{R_B}{r_{B0}} \right)^2 P_{20}(\cos \theta_B) \right) \right\} dt + \mathcal{O}(1.10 \times 10^{-16})(t^* - t_0), \quad (60)$$

with the representation of the motion of the clock with respect to the BCRS given as below

$$\bar{\mathbf{x}}_0(\tau) = \mathbf{x}_0(t^*), \quad (61)$$

that may be solved either numerically or analytically, in the analogy to the approach used in (3)–(4). For direct transformations (56), one should integrate the integral either numerically or analytically. For the inverse transformation (59), to express the right-hand members in terms of τ , one must obtain the function $t^* = t^*(\tau)$ by inverting the equation (60), also either numerically or analytically.

III. BCRS IMPLEMENTATION AND FRAME-CLOSURE VALIDATION FOR GNSS DYNAMICS

In this Section, we validate the BCRS-native implementation and the GCRS \leftrightarrow BCRS state transformations developed in Sec. IID via an internal *frame-closure* experiment. Specifically, we compare a GPS-like trajectory obtained by integrating the TT-compatible GCRS equations of motion to the trajectory obtained by (i) transforming the same initial state into the TDB-compatible BCRS, (ii) integrating the corresponding barycentric equations of motion, and (iii) transforming the resulting state back into the GCRS at each epoch. The resulting closure residuals quantify numerical and modeling consistency of the transformation chain and force models; they are not intended as an assessment of end-to-end user positioning accuracy from observations.

For completeness, we summarize the equations of motion used in each frame and highlight the treatment of the dominant Newtonian, post-Newtonian, and geopotential terms needed to reproduce the closure experiment.

A. Equations of motion in the scaled TDB-compatible BCRS

1. BCRS metric in the mass monopole approximation

For many applications, it suffices to consider only the mass monopoles of all solar system bodies, retaining solely the masses which represents the mass monopole approximation of the BCRS metric, for a system of N point-like gravitational sources in four dimensions is outlined in [1]:

$$\begin{aligned} g_{00} &= 1 - \frac{2}{c^2} \sum_{j \neq i} \frac{\mu_j}{r_{ij}} + \frac{2\beta}{c^4} \left[\sum_{j \neq i} \frac{\mu_j}{r_{ij}} \right]^2 - \frac{1+2\gamma}{c^4} \sum_{j \neq i} \frac{\mu_j \dot{r}_j^2}{r_{ij}} + \frac{2(2\beta-1)}{c^4} \sum_{j \neq i} \frac{\mu_j}{r_{ij}} \sum_{k \neq j} \frac{\mu_k}{r_{jk}} - \frac{1}{c^4} \sum_{j \neq i} \mu_j \frac{\partial^2 r_{ij}}{\partial t^2} + \mathcal{O}(c^{-5}), \\ g_{0\alpha} &= \frac{2(\gamma+1)}{c^3} \sum_{j \neq i} \frac{\mu_j \dot{\mathbf{r}}_j^\alpha}{r_{ij}} + \mathcal{O}(c^{-5}), \quad g_{\alpha\beta} = \gamma_{\alpha\beta} \left(1 + \frac{2\gamma}{c^2} \sum_{j \neq i} \frac{\mu_j}{r_{ij}} \right) + \mathcal{O}(c^{-4}), \end{aligned} \quad (62)$$

where the indices j and k refer to the N bodies, with k including body i , whose motion is being investigated. The gravitational constant for body j , denoted as μ_j , is defined as $\mu_j = Gm_j$, where G is the universal Newtonian gravitational constant, and m_j is the isolated rest mass of body j . Additionally, the vector \mathbf{r}_i represents the barycentric radius-vector of this body. The vector $\mathbf{r}_{ij} = \mathbf{r}_j - \mathbf{r}_i$ points from body i to body j , $r_{ij} = |\mathbf{r}_j - \mathbf{r}_i|$, and the vector $\mathbf{n}_{ij} = \mathbf{r}_{ij}/r_{ij}$ is the unit vector along this direction.

Furthermore, in (62), we have reinstated the parameterized post-Newtonian (PPN) parameters [36], which have been adapted to relativistic reference frames in [37]. The two PPN parameters, γ and β , have specific physical interpretations: γ quantifies the curvature of space-time produced by a unit rest mass, while β quantifies the non-linearity in the superposition of gravitational fields in gravity theory. In general relativity, $\gamma = \beta = 1$, and the other eight parameters are absent, situating the theory within a two-dimensional theoretical framework.

2. Equations of motion in BCRS: point-mass approximation

The barycentric metric given by (62) may be used to derive the post-Newtonian EIH equations of motion for a system of mass monopoles. These equations form the basis of modern solar system ephemerides. The relevant point-mass Newtonian and relativistic perturbative accelerations in the TDB-compatible BCRS are used to describe the motion of spacecraft in the solar system, including Earth orbiters and the Moon. The corresponding EIH equations are given as follows [1]:

$$\begin{aligned} \ddot{\mathbf{r}}_i &= \sum_{j \neq i} \frac{\mu_j (\mathbf{r}_j - \mathbf{r}_i)}{r_{ij}^3} \left\{ 1 - \frac{2(\beta+\gamma)}{c^2} \sum_{l \neq i} \frac{\mu_l}{r_{il}} - \frac{2\beta-1}{c^2} \sum_{k \neq j} \frac{\mu_k}{r_{jk}} + \gamma \left(\frac{\dot{r}_i}{c} \right)^2 + (1+\gamma) \left(\frac{\dot{r}_j}{c} \right)^2 - \frac{2(1+\gamma)}{c^2} (\dot{\mathbf{r}}_i \cdot \dot{\mathbf{r}}_j) - \right. \\ &\quad \left. - \frac{3}{2c^2} \left[\frac{(\mathbf{r}_i - \mathbf{r}_j) \cdot \dot{\mathbf{r}}_j}{r_{ij}} \right]^2 + \frac{1}{2c^2} ((\mathbf{r}_j - \mathbf{r}_i) \cdot \ddot{\mathbf{r}}_j) \right\} + \frac{1}{c^2} \sum_{j \neq i} \frac{\mu_j}{r_{ij}^3} \left\{ (\mathbf{r}_i - \mathbf{r}_j) \cdot \left((2+2\gamma)\dot{\mathbf{r}}_i - (1+2\gamma)\dot{\mathbf{r}}_j \right) \right\} (\dot{\mathbf{r}}_i - \dot{\mathbf{r}}_j) + \\ &\quad + \frac{3+4\gamma}{2c^2} \sum_{j \neq i} \frac{\mu_j \ddot{\mathbf{r}}_j}{r_{ij}} + \sum_{m=1}^3 \frac{\mu_m (\mathbf{r}_m - \mathbf{r}_i)}{r_{im}^3} + \sum_{c,s,m} \mathbf{F} + \mathcal{O}(c^{-4}). \end{aligned} \quad (63)$$

The first term in (63) represents the Newtonian gravitational acceleration, which must be computed using barycentric TDB-compatible quantities. The subsequent terms are the post-Newtonian contributions. The penultimate term on the right-hand side of (63) refers to the ‘Big3’ asteroids—Ceres, Pallas, and Vesta—using the index m . The final term accounts for forces on the Earth, Moon, and Mars from 297 other asteroids, which are grouped into three taxonomic classes (C, S, M), see [38] for details. For a planetary orbiter, it is usual to integrate the difference between the orbiter’s acceleration and the planet’s acceleration, both derived from the EIH equations. Typically, only the relativistic corrective terms with the index j matching either the central planet or the Sun have significant effects.

3. Light time equation

To determine the orbits of planets and spacecraft, one must also account for the propagation of EM signals between any two points in space. The corresponding light-time equation is derived from the metric tensor in (62) as follows:

$$t_2 - t_1 = \frac{r_{12}}{c} + (1+\gamma) \sum_B \frac{GM_B}{c^3} \ln \left[\frac{r_1^B + r_2^B + r_{12}}{r_1^B + r_2^B - r_{12}} \right] + \mathcal{O}(c^{-5}), \quad (64)$$

where t_1 and t_2 refer to the signal's emission and reception coordinate times, respectively, $\mathbf{r}_1 \equiv \mathbf{r}(t_1)$ and $\mathbf{r}_2 \equiv \mathbf{r}(t_2)$ are the barycentric position vectors of emitter and receiver, and $r_{12} \equiv |\mathbf{r}_2 - \mathbf{r}_1|$. For each gravitating body \mathbf{B} in the sum, $r_1^{\mathbf{B}} \equiv |\mathbf{r}_1 - \mathbf{x}_{\mathbf{B}}(t_1)|$ and $r_2^{\mathbf{B}} \equiv |\mathbf{r}_2 - \mathbf{x}_{\mathbf{B}}(t_2)|$ are the emitter/receiver distances to \mathbf{B} . The Shapiro term is proportional to $(1 + \gamma)$, with $\gamma = 1$ in general relativity.

The Shapiro time delay is proportional to $(1 + \gamma)$. The average solar potential at a distance of 1 AU is $\langle U \rangle / c^2 = 0.99 \times 10^{-8}$. The mean delay caused by the Sun for GPS signals is ~ 2.66 ns, equivalent to ~ 79.8 cm. The annual variation is ± 7 mm. The delay due to Earth's gravity can reach up to 42.3 ps (or ~ 1.3 cm), and it varies with the elevation angle. Therefore, only the Sun and Earth must be included in the model (64). At L-band, solar plasma delay is negligible except near conjunction; apply standard transformations for troposphere/ionosphere in the observable model. Most of the solar term behaves as an overall scale in range and cancels in differenced observables, but should be retained for absolute light-time consistency at the centimeter level.

For increased fidelity near conjunctions, evaluate the Shapiro term in (64) with retarded ephemeris positions of gravitating bodies \mathbf{B} :

$$\mathbf{x}_{\mathbf{B}}^{\text{ret}}(t_i) \simeq \mathbf{x}_{\mathbf{B}}(t_i) - \frac{r_{\mathbf{B},i}}{c} \mathbf{v}_{\mathbf{B}}(t_i), \quad r_{\mathbf{B},i} \equiv \|\mathbf{r}_i - \mathbf{x}_{\mathbf{B}}^{\text{ret}}(t_i)\|, \quad i \in \{1, 2\}.$$

This accounts for leading $\mathcal{O}(v_{\mathbf{B}}/c)$ corrections without changing the observable interface. The light-time and its derivatives used here are consistent with the time-transfer-function (TTF) formalism; see e.g., [39] for the moving-axisymmetric-body generalization used in interplanetary radioscience.

When either endpoint lies on the rotating Earth, the one-way coordinate light-time acquires the Sagnac correction due to the rotation vector $\boldsymbol{\Omega}_{\oplus}$,

$$\Delta t_{\text{sag}} = \frac{1}{c^2} (\boldsymbol{\Omega}_{\oplus} \cdot [\mathbf{r}_{\mathbf{R}}(t_r) \times \mathbf{r}_{\mathbf{T}}(t_e)]), \quad (65)$$

so the total is $\Delta t = \Delta t_{\text{geom}} + \Delta t_{\text{Shapiro}} + \Delta t_{\text{sag}}$, with Δt_{geom} and $\Delta t_{\text{Shapiro}}$ as in (64). Numerically, for a typical GNSS MEO geometry with $|\mathbf{r}_{\mathbf{R}}| \approx 6378$ km, $|\mathbf{r}_{\mathbf{T}}| \approx 26,560$ km, and $|\boldsymbol{\Omega}_{\oplus}| = 7.292115 \times 10^{-5} \text{ s}^{-1}$, one finds $|\Delta t_{\text{sag}}| \lesssim 1.4 \times 10^{-7} \text{ s}$ (≈ 41 m in range), hence mandatory for centimeter modeling of ground links [40]. The term (65) leads to a correction

$$\frac{\partial}{\partial t_r} \Delta t_{\text{sag}} = \frac{1}{c^2} \left(\boldsymbol{\Omega}_{\oplus} \cdot \left([\mathbf{v}_{\mathbf{R}}(t_r) \times \mathbf{r}_{\mathbf{T}}(t_e)] - [\mathbf{v}_{\mathbf{T}}(t_e) \times \mathbf{r}_{\mathbf{R}}(t_r)] \right) \right), \quad (66)$$

that is required wherever one forms two-way frequency/phase models. For a rotating ground site this term is at the $10^{-12} - 10^{-11}$ fractional level for L-band.

4. Frequency transfer observable at $\mathcal{O}(c^{-3})$

For one-way transfer from emitter \mathbf{A} to receiver \mathbf{B} ,

$$\frac{\nu_{\mathbf{A}}}{\nu_{\mathbf{B}}} = \frac{(u^0)_{\mathbf{A}}}{(u^0)_{\mathbf{B}}} \frac{q_{\mathbf{A}}}{q_{\mathbf{B}}} + \mathcal{O}(c^{-4}), \quad (67)$$

where the ratio $q_{\mathbf{A}}/q_{\mathbf{B}}$ follows from differentiating the light-time equation (64) with respect to emission time, retaining terms through $\mathcal{O}(c^{-3})$ [10, 41].

For GNSS applications the relevant observable is the one-way downlink. An explicit post-Newtonian expansion of the propagation factor $q_{\mathbf{A}}/q_{\mathbf{B}}$ through $\mathcal{O}(c^{-3})$, consistent with Eq. (64), is given in Ref. [41] (see also Refs. [1, 39]). In our implementation we compute $(u^0)_{\mathbf{A}}$ and $(u^0)_{\mathbf{B}}$ from the adopted metric and obtain $q_{\mathbf{A}}/q_{\mathbf{B}}$ from the derivative $d(t_2 - t_1)/dt_1$ evaluated along the modeled light-time solution. These expressions are consistent with our light-time (64) and close the model for range-rate and frequency transfer at the level needed for 10^{-16} work.

B. Equations of motion in the scaled TT-compatible GCRS

1. GCRS: Practically-relevant formulation

In practical GCRS implementations, one includes all post-Newtonian terms up to $\mathcal{O}(c^{-4})$ in G_{00} , $\mathcal{O}(c^{-3})$ in $G_{0\alpha}$, and $\mathcal{O}(c^{-2})$ in $G_{\alpha\beta}$, but discards any metric perturbations smaller than 5×10^{-18} . Accordingly, the metric tensor of

GCRS (see [8, 21]) retaining only $|\delta G_{mn}| \gtrsim 5 \times 10^{-18}$, sufficient for high-precision time-keeping applications, becomes

$$G_{00}(T, \mathbf{X}) = 1 - \frac{2}{c^2} \left\{ W_E(T, \mathbf{X}) + W_{\text{tid}}(T, \mathbf{X}) \right\} + \frac{2}{c^4} W_E^2(T, \mathbf{X}) + \mathcal{O}(c^{-5}; 6.61 \times 10^{-25}), \quad (68)$$

$$G_{0\alpha}(T, \mathbf{X}) = -\frac{2G}{c^3} \frac{[\mathbf{S}_E \times \mathbf{X}]_\alpha}{R^3} + \mathcal{O}(c^{-5}; 2.79 \times 10^{-19}), \quad (69)$$

$$G_{\alpha\beta}(T, \mathbf{X}) = \gamma_{\alpha\beta} \left(1 + \frac{2}{c^2} \left\{ W_E(T, \mathbf{X}) + W_{\text{tid}}(T, \mathbf{X}) \right\} \right) + \mathcal{O}(c^{-4}; 5.57 \times 10^{-20}), \quad (70)$$

where $S_E \simeq 5.86 \times 10^{33} \text{ kg m}^2/\text{s}$ is the Earth spin vector moment. Also, $W_E(T, \mathbf{X})$ is the Earth's gravitational potential

$$W_E(T, \mathbf{X}) = \frac{GM_E}{R} \left\{ 1 + \sum_{\ell=2}^{\infty} \sum_{m=0}^{\ell} \left(\frac{R_E}{R} \right)^\ell P_{\ell m}(\cos \theta) \left(C_{\ell m}^E(T, R) \cos m\phi + S_{\ell m}^E(T, R) \sin m\phi \right) \right\} + \mathcal{O}(c^{-4}), \quad (71)$$

where M_E and R_E are the Earth's mass and equatorial radius, respectively, while $P_{\ell k}$ are the associated Legendre polynomials [42]. $W_{\text{tid}}(T, \mathbf{X})$ is the Newtonian the tidal potential by external bodies

$$W_{\text{tid}}(T, \mathbf{X}) = U_{\text{ext}}(\mathbf{x}_E + \mathbf{X}) - U_{\text{ext}}(\mathbf{x}_E) - (\mathbf{X} \cdot \nabla U_{\text{ext}}(\mathbf{x}_E)), \quad (72)$$

where $\mathbf{r}_{BE} = \mathbf{x}_E - \mathbf{x}_B$ is the vector connecting the center of mass of body B with that of the Earth, with $r_{BE} = |\mathbf{r}_{BE}|$ and $\mathbf{n}_{BE} = \mathbf{r}_{BE}/r_{BE}$, also $\hat{\mathbf{X}} = \mathbf{X}/X$ and $\cos \theta_{BE} = (\mathbf{n}_{BE} \cdot \hat{\mathbf{X}})$, with $P_\ell(\cos \theta)$ being the Legendre polynomials. Naturally, the quadratic term (i.e., $\sim \mathcal{O}(X^2)$) in the resulting expression for W_{tidal} is the dominant one.

The error bounds in (68)–(70) are due to the dominant omitted corrections evaluated at GPS altitude, specifically: $\delta G_{00}^{(\text{mix})} = -4c^{-4} W_E W_{\text{tid}} \simeq 4c^{-4} (GM_E/r_{\text{GPS}}) (GM_S/\text{AU}^3 + Gm_M/r_{\text{EM}}^3) r_{\text{GPS}}^2 \simeq 6.61 \times 10^{-25}$; $\delta G_{0\alpha}^{(\text{tid})} = -4c^{-3} W_{\text{tid}}^\alpha \simeq 4c^{-3} (GM_M/r_{\text{EM}}^3) v_M r_{\text{GPS}}^2 \simeq 2.79 \times 10^{-19}$; and $\delta G_{\alpha\beta}^{(2\text{PN})} = \gamma_{\alpha\beta} \frac{3}{2} c^{-4} W_E^2 \simeq \frac{3}{2} c^{-4} (GM_E/r_{\text{GPS}})^2 \simeq 4.78 \times 10^{-20}$, see details in [21]. Although we evaluated the metric components in (68)–(70) at GPS altitude (i.e., where tidal contributions exceed those at the surface), these expressions remain valid for all Earth-orbit regimes from MEO through GEO.

2. Equations of motion in the GCRS

The trajectory of an Earth satellite in GCRS is governed by the following equation of motion [1, 13, 32, 40, 43]:

$$\ddot{\mathbf{r}} = \ddot{\mathbf{r}}_E + \ddot{\mathbf{r}}_{E,J_2} + \ddot{\mathbf{r}}_{\text{tidal}} + \ddot{\mathbf{r}}_{\text{GR}} + \ddot{\mathbf{r}}_{\text{SRP}} + \ddot{\mathbf{r}}_{\text{Elast}} + \ddot{\mathbf{r}}_{\text{Erads}} + \ddot{\mathbf{r}}_{\text{custom}}, \quad (73)$$

where $\ddot{\mathbf{r}}_E$ is the Newtonian acceleration due to the gravity field of the Earth²; $\ddot{\mathbf{r}}_{E,J_2}$ is the acceleration due to Earth's oblateness; $\ddot{\mathbf{r}}_{\text{tidal}}$ is the acceleration due to the tidal gravity field induced by the Sun, Moon and Venus; $\ddot{\mathbf{r}}_{\text{GR}}$ is the acceleration due to general relativity; $\ddot{\mathbf{r}}_{\text{SRP}}$ is the acceleration due to direct/indirect solar radiation pressure; $\ddot{\mathbf{r}}_{\text{Elast}}$ is the acceleration due to elastic Earth response, pole, and ocean tides; $\ddot{\mathbf{r}}_{\text{Erads}}$ is the acceleration due to Earth albedo and infra-red (IR) radiation; and $\ddot{\mathbf{r}}_{\text{custom}}$ is the acceleration due to any custom force model. Note that all quantities (positions, accelerations, distances, mass parameters) in (73) are TT-compatible.

The acceleration of a spacecraft at \mathbf{r} , due to the Earth's gravity field in (73) is computed as usual

$$\ddot{\mathbf{r}}_E = \nabla U_E(\mathbf{r}) + \mathcal{O}(c^{-4}) = -\frac{GM_E}{r^3} \mathbf{r} \left(1 + \mathcal{O}\left(\frac{R_E^2}{r^2}\right) \right) \simeq -\frac{GM_E}{a^2} \mathbf{n}_r \approx 0.57 \text{ m/s}^2, \quad (74)$$

where $\mathbf{a} = a\mathbf{n}_r$ is the semi-major axis of the spacecraft orbit, $\mathbf{n}_r = \mathbf{r}/r$ is the unit vector in the direction of the spacecraft from the GCRS. In this estimate, we truncated the Earth relativistic gravitational potential $U_E(\mathbf{x}) \equiv W_E(T, \mathbf{X})$ from (71) to the monopole term. Clearly, this is the dominant term in the equations of motion of an Earth-orbiting satellite (73).

Let $\mu_E = GM_E$, R_E the Earth's mean equatorial radius, $J_{2,E}$ the quadrupole coefficient, $\hat{\mathbf{r}} = \mathbf{r}/r$, and $\hat{\mathbf{S}}$ the unit spin axis of the Earth. The 1PN gravitoelectric acceleration due to the oblateness is

$$\begin{aligned} \ddot{\mathbf{r}}_{E,J_2} = & \frac{3J_{2,E} \mu_E R_E^2}{2c^2 r^4} \left([5 \hat{\mathbf{r}}(\hat{\mathbf{S}} \cdot \hat{\mathbf{r}})^2 - 2 \hat{\mathbf{S}}(\hat{\mathbf{S}} \cdot \hat{\mathbf{r}}) - \hat{\mathbf{r}}] [v^2 - \frac{4\mu_E}{r}] - \right. \\ & \left. - 4[5(\hat{\mathbf{r}} \cdot \mathbf{v})(\hat{\mathbf{S}} \cdot \hat{\mathbf{r}})^2 - 2(\hat{\mathbf{S}} \cdot \mathbf{v})(\hat{\mathbf{S}} \cdot \hat{\mathbf{r}}) - (\hat{\mathbf{r}} \cdot \mathbf{v})] \mathbf{v} - \frac{4\mu_E}{r} [3(\hat{\mathbf{S}} \cdot \hat{\mathbf{r}})^2 - 1] \hat{\mathbf{r}} \right). \end{aligned} \quad (75)$$

² Note that, for convenience, we are using lowercase letters to denote vectors in the GCRS, rather than uppercase letters.

In the worst-case orientation and using $J_{2,E} = 1.08263 \times 10^{-3}$, $R_E = 6378$ km, $\mu_E = 3.986 \times 10^{14}$ m³s⁻², this acceleration was evaluated to contribute: LEO: $\sim 7 \times 10^{-11}$ m/s², MEO: $\sim 10 \times 10^{-13}$ m/s², cislunar: $\sim 5 \times 10^{-16}$ m/s². Thus, for LEO its omission biases precise orbit and gravity solutions, while for MEO it is small but systematic. A useful scaling is $\ddot{\mathbf{r}}_{EJ_{2,E}} \propto r^{-4}$, so the effect rapidly decreases for higher Earth orbits. As a rough displacement scale over a one-day arc, $\frac{1}{2}|\ddot{\mathbf{r}}|\Delta t^2$ with $\Delta t = 86400$ s gives ~ 0.3 m (LEO, using 7×10^{-11} m/s²) and ~ 4 mm (GPS-like MEO, using 1×10^{-12} m/s²); at lunar distance it falls below the micron level. Accordingly, the 1PN J_2 term is mandatory for LEO POD, can matter for mm-level MEO processing, and is negligible for lunar-distance dynamics.

The tidal acceleration due to the gravity fields of the Sun, Venus and Moon are also well known. Using $u_E^{\text{tidal}}(\mathbf{x}) \equiv W_{\text{tidal}}(\mathbf{x})$ from (72), we compute it as usual:

$$\begin{aligned} \ddot{\mathbf{r}}_{\text{tidal}} &= \nabla u_E^{\text{tidal}}(\mathbf{x}) + \mathcal{O}\left(\frac{x^3}{r_{\text{BE}}^4}, c^{-2}\right) \simeq \sum_{b \neq E} \frac{GM_b}{r_{\text{BE}}^3} \left(3(\mathbf{n}_{\text{BE}} \cdot \mathbf{r})\mathbf{n}_{\text{BE}} - \mathbf{r}\right) \leq \\ &\leq \frac{2GM_S a}{a_E^3} (\mathbf{n}_S \cdot \mathbf{n}_r) \mathbf{n}_S + \frac{2GM_M a}{a_M^3} (\mathbf{n}_M \cdot \mathbf{n}_r) \mathbf{n}_M + \frac{2GM_V a}{a_V^3} (\mathbf{n}_V \cdot \mathbf{n}_r) \mathbf{n}_V \approx \\ &\approx 2.11 \times 10^{-6} \text{ m/s}^2 + 4.59 \times 10^{-6} \text{ m/s}^2 + 2.45 \times 10^{-10} \text{ m/s}^2, \end{aligned} \quad (76)$$

where a_E, e_E , and \mathcal{E}_E and a_V, e_V , and \mathcal{E}_V are the semi-major axis, eccentricity and eccentric anomaly characterizing the heliocentric orbits of the Earth and Venus correspondingly, while a_M, e_M , and \mathcal{E}_M , are the same quantities for the geocentric orbit of the Moon. We will use the value of $a_M = 384,400$ km to denote the Earth-Moon mean distance.

In addition, we estimate the maximal accelerations from the tides introduced by Jupiter and Saturn:

$$|\ddot{\mathbf{r}}_{\text{tidal}}^J| \lesssim \frac{2GM_J a}{(a_J - a_E)^3} \approx 2.70 \times 10^{-11} \text{ m/s}^2, \quad |\ddot{\mathbf{r}}_{\text{tidal}}^{\text{Sa}}| \lesssim \frac{2GM_{\text{Sa}} a}{(a_{\text{Sa}} - a_E)^3} \approx 9.52 \times 10^{-13} \text{ m/s}^2, \quad (77)$$

with contributions from Uranus, Neptune being below 10^{-14} m/s². Note that these tidal forces are not accounted for in the equations of motion used to process GPS observables. Due to the long orbital periods of these planets, they contribute a nearly constant background that is removed along with other constant terms during data analysis.

The relativistic corrections to the accelerations of Earth satellites written in a local inertial GCRS that is kinematically non-rotating read as [44]:

$$\begin{aligned} \ddot{\mathbf{r}}_{\text{GR}} &= \frac{GM_E}{c^2 r^3} \left\{ \left[2(\beta + \gamma) \frac{GM_E}{r} - \gamma \dot{\mathbf{r}}^2 \right] \mathbf{r} + 2(1 + \gamma)(\mathbf{r} \cdot \dot{\mathbf{r}}) \dot{\mathbf{r}} \right\} + \\ &+ (1 + \gamma) \frac{GM_E}{c^2 r^3} \left[\frac{3}{r^2} [\mathbf{r} \times \dot{\mathbf{r}}](\mathbf{r} \cdot \mathbf{S}_E) + [\dot{\mathbf{r}} \times \mathbf{S}_E] \right] + (1 + 2\gamma) \frac{GM_S}{c^2 r_E^3} [[\mathbf{r}_E \times \dot{\mathbf{r}}_E] \times \dot{\mathbf{r}}], \end{aligned} \quad (78)$$

where GM_E is the standard Earth gravitation product; GM_S is the standard Sun gravitation product; β, γ are PPN parameters equal to 1 in GR; c is the speed of light; $\mathbf{r}, \dot{\mathbf{r}}$ are the position and velocity of a satellite with respect to the geocenter; $\mathbf{r}_E, \dot{\mathbf{r}}_E$ are the position and velocity of the Earth with respect to the Sun; \mathbf{S}_E is the Earth's spin moment (angular momentum per unit of mass). Introducing \mathcal{R} as the rotation matrix transformations ECEF \rightarrow inertial, we write $\mathbf{S}_E \simeq 0.33068 R_E^2 \omega_E \mathcal{R} \hat{\mathbf{z}}$.

The first line describes the so-called Schwarzschild term [45, 46], the next term is the frame-dragging gravitomagnetic Lense-Thirring effect [47], whereas the third corresponds to the de Sitter effect [48]. Other relativistic effects are related to, e.g., other celestial bodies, which can be approximated as small corrections to the non-relativistic tidal forces, Thomas precession, or Earth's oblateness quadruple term; however, they are currently not considered in the precise GNSS orbit solutions, due to their very small magnitudes [7, 32, 43, 44, 49].

We evaluate the Schwarzschild term in (78) as:

$$\ddot{\mathbf{r}}_{\text{Sch}} = \frac{GM_E}{c^2 r^3} \left\{ \left[2(\beta + \gamma) \frac{GM_E}{r} - \gamma \dot{\mathbf{r}}^2 \right] \mathbf{r} + 2(1 + \gamma)(\mathbf{r} \cdot \dot{\mathbf{r}}) \dot{\mathbf{r}} \right\} \simeq \frac{3(GM_E)^2}{c^2 a^3} \frac{1}{3} (2\beta + \gamma) \mathbf{n}_r \leq 2.83 \times 10^{-10} \text{ m/s}^2. \quad (79)$$

For GNSS MEO orbit determination, planetary tidal terms beyond Sun/Moon are typically negligible at the cm level over daily arcs and are largely absorbed by empirical parameters; Eq. (77) quantifies that even worst-case Jupiter/Saturn tidal accelerations remain $\lesssim 10^{-11}$ m/s².

Next, we evaluate the frame-dragging gravitomagnetic Lense-Thirring effect in (78):

$$\ddot{\mathbf{r}}_{\text{LT}} = (1 + \gamma) \frac{GM_E}{c^2 r^3} \left[\frac{3}{r^2} [\mathbf{r} \times \dot{\mathbf{r}}](\mathbf{r} \cdot \mathbf{S}_E) + [\dot{\mathbf{r}} \times \mathbf{S}_E] \right] \simeq 1.98 \left(\frac{GM_E}{a} \right)^{\frac{3}{2}} \frac{R_E^2 \omega_E}{c^2 a^2} \frac{1}{2} \sin 2i_0 \sin i_{\text{ec1}} \leq 0.98 \times 10^{-12} \text{ m/s}^2, \quad (80)$$

where we used the unit vectors $\mathbf{n}_{[\mathbf{r} \times \dot{\mathbf{r}}]} = [\mathbf{r} \times \dot{\mathbf{r}}]/|\mathbf{r} \times \dot{\mathbf{r}}|$, $\mathbf{n}_r = \mathbf{r}/r$ and $\mathbf{n}_v = \mathbf{v}/v$. In addition, we introduce the unit vector $\mathbf{n}'_z = \hat{\mathbf{T}}\mathbf{n}_z$ relating the Earth's angular momentum with the direction to the north pole. Also, i_0 is the spacecraft's orbital inclination, $i_0 = 55^\circ$ for GPS orbits, and where $i_{\text{ec1}} = 23.5^\circ$ is Earth's axial tilt.

Finally, we consider the de Sitter effect due to the Sun in (78):

$$\ddot{\mathbf{r}}_{\text{dS}}^{\text{S}} = (1 + 2\gamma) \frac{GM_{\text{S}}}{c^2 r_{\text{E}}^3} [[\mathbf{r}_{\text{E}} \times \dot{\mathbf{r}}_{\text{E}}] \times \dot{\mathbf{r}}] \simeq \frac{3}{c^2 a_{\text{E}}} \left(\frac{GM_{\text{S}}}{a_{\text{E}}} \right)^{\frac{3}{2}} \sqrt{\frac{GM_{\text{E}}}{a}} \frac{1}{3} (1 + 2\gamma) \sin i_{\text{ec1}} \leq 8.92 \times 10^{-12} \text{ m/s}^2. \quad (81)$$

The de Sitter term written here is the dominant solar contribution for Earth satellites. Quantitatively, the dominant contribution to the geodetic (de Sitter) term in Eq. (78) is solar. For a near-Earth satellite, a simple magnitude estimate gives

$$\frac{a_{\text{dS}}^{\text{Moon}}}{a_{\text{dS}}^{\text{Sun}}} \sim \frac{GM_{\text{M}} v_{\text{EM}}/r_{\text{EM}}^2}{GM_{\text{S}} v_{\text{ES}}/r_{\text{ES}}^2} \approx 2 \times 10^{-4},$$

where $(\mathbf{r}_{\text{ES}}, \mathbf{v}_{\text{ES}})$ and $(\mathbf{r}_{\text{EM}}, \mathbf{v}_{\text{EM}})$ denote the Earth–Sun and Earth–Moon relative state vectors. Thus, if the solar de Sitter acceleration is $\sim 10^{-11} \text{ m/s}^2$ (81), the corresponding Moon term is $\lesssim 10^{-15} \text{ m/s}^2$, and other planets are smaller still.

Thus, relativistic contributions presented above are important and must be kept in the model.

3. Transforming equations of motion from GCRS to BCRS

The metric tensor (68)–(70) along with the gravitational potentials (71)–(72) describes spacetime in the GCRS, which we adopt to formulate the relativistic model for timing and frequency observables. Detailed derivations of the GCRS formulation can be found in [7, 10, 11, 50]. As a result, within the local GCRS, the following gravitational accelerations due to mass monopoles must be considered:

- The Newtonian gravitational acceleration from the Earth, given by (74).
- The relativistic correction to the Earth's gravitational acceleration, provided by the leading term in (78).
- The accelerations associated with De Sitter and Lense–Thirring precessions, given by the 2-nd and 3-rd terms in (78).
- The third-body Newtonian acceleration due to tidal effects from all other solar system bodies, described by (76).

Accurate evaluation of third-body accelerations in a TT-compatible GCRS propagation requires consistent use of barycentric ephemerides (typically delivered in TDB-compatible form) and the corresponding TT↔TDB time mapping. The procedure, as outlined in [1], Sec. 4.5.1, involves the following steps:

- Convert the integration time from TT to TDB along the spacecraft's worldline using Eqs. (12)–(15). Although TT – TDB is periodic with amplitude $\lesssim 2 \text{ ms}$, an unconverted ephemeris query can correspond to a barycentric epoch error that maps to $v_{\text{E}} \Delta t \lesssim 60 \text{ m}$ and can produce $\sim \text{cm}$ -level differences over a 24 h arc in third-body accelerations; we therefore treat the time-scale conversion as part of the deterministic force model.
- Obtain the TDB-compatible BCRS state vectors for both the Earth and the third body from the planetary ephemeris at the corresponding TDB epoch.
- Determine the position vectors from the spacecraft to the third body and from Earth to the third body using the TDB-compatible BCRS states of the Earth and the third body, combined with the TT-compatible GCRS state of the spacecraft.
- Compute the third-body acceleration using these position vectors and the mass parameter of the third body from the BCRS, ensuring compatibility with the TDB time scale.
- Apply a scaling factor to the computed third-body acceleration by multiplying it by $(1 - L_{\text{C}})$, where L_{C} accounts for the relativistic corrections. *Implementation guard:* Apply the $(1 - L_{\text{C}})$ factor only if the third-body term was built from TT-compatible constants. If you compute the term with TDB-compatible states and GM values (e.g., DE440), do not apply an additional $(1 - L_{\text{C}})$; the scaling in Sec. IID already accounts for it.

Note that relativistic corrections to third-body perturbations are typically small and often disregarded. The main effect is due to the Sun’s gravitational influence, with smaller contributions from other planets, causing the local inertial frames near Earth to experience De Sitter precession relative to the BCRS in the TDB frame. Nevertheless, the TT-compatible GCRS remains kinematically non-rotating relative to the TDB-compatible BCRS. This non-rotation creates a non-inertial reference frame, requiring the inclusion of Coriolis acceleration.

The De Sitter acceleration (81), is a relativistic correction to 3rd-body acceleration and is implicitly included when using the EIH equations in the BCRS (see [1], Sec. 4.4.2). It is important to note that Lense-Thirring precession (80) (see also [1], Secs. 4.4.3 and 4.5.4), is an independent effect caused by the angular momentum of the Earth (or a planet) and is not included in the EIH equations. The full set of relativistic correction terms is provided in (78).

4. Considering the gravitational harmonics of the Earth

The Earth’s motion around the Sun induces relativistic distortions in the gravitational spherical harmonics when observed in the BCRS. These distortions complicate the accurate computation of accelerations arising from these harmonics within the barycentric system. To mitigate these effects, it is necessary to apply relativistic corrections, which involve several key steps detailed in [1], Sec. 4.4.5:

- Transform the spacecraft’s position vector from the TDB-compatible BCRS to the TT-compatible GCRS using a Lorentz transformation (refer to [1], Eq. (4-11)).
- Calculate the acceleration due to gravitational spherical harmonics in the TT-compatible GCRS.
- Convert the computed acceleration back to the barycentric frame using the method outlined in [1], Eq. (4-55).

This method can be applied to other planets as well. Given the relativistic distortions present in the barycentric reference frame, performing spherical harmonic expansions in a planetocentric system provides improved precision. Additionally, it is imperative to confirm that the reference radius and mass parameters used in the spherical harmonic expansion are properly scaled to account for relativistic effects. If these parameters do not reflect the appropriate relativistic scaling, they must be adjusted to ensure accuracy in the calculations.

This method accounts for the relativistic adjustments that arise from transformations between different space-time coordinate systems. Incorporating these corrections significantly improves the precision of the calculated acceleration due to the geopotential in the geocentric reference frame. Notably, the relativistic correction associated with the acceleration from Earth’s quadrupole moment, J_2 , is extensively discussed in [51], Sec. 4.2.3.

C. Practical implementation and validation

In this Section, we outline the validation tests performed to verify the proper implementation of the EIH equations within the interplanetary orbit determination system used by GNSS spacecraft. The testing involved comparing the accelerations computed in the BCRS with those calculated in the GCRS. To enable this comparison, the accelerations derived in the GCRS were transformed into the BCRS using a series of relativistic transformations described in Sec. IID. This approach ensures that the system accurately incorporates the relativistic effects necessary for precise navigation and tracking of GNSS spacecraft. Table V shows configuration used for the closure test.

We define the *frame-closure residuals* as

$$\Delta\mathbf{r}(T) \equiv \mathbf{X}_{\text{BCRS} \rightarrow \text{GCRS}}(T) - \mathbf{X}_{\text{GCRS}}(T), \quad \Delta\dot{\mathbf{r}}(T) \equiv \dot{\mathbf{X}}_{\text{BCRS} \rightarrow \text{GCRS}}(T) - \dot{\mathbf{X}}_{\text{GCRS}}(T), \quad (82)$$

where $\mathbf{X}_{\text{GCRS}}(T)$ is obtained by integrating the GCRS equations of motion, and $\mathbf{X}_{\text{BCRS} \rightarrow \text{GCRS}}(T)$ is obtained by transforming the initial state into the BCRS, integrating the corresponding barycentric equations of motion, and transforming the state back into the GCRS at each epoch. Figure 1 shows the components of $\Delta\mathbf{r}(t)$ in the local radial/along-track/cross-track frame.

Table VI provides a minimal *template* for regression tests of the GCRS \leftrightarrow BCRS transformations. For externally reproducible validation, generate the numerical values using a specified ephemeris (e.g., DE440), Earth-orientation series, reference epoch, and double-precision arithmetic, and publish the resulting vectors alongside the expected tolerances. States are referenced to DE440 (TDB argument) and ITRF2020-to-GCRS realized by IERS (2010), [5]. Use double precision (or higher) and report agreement to the thresholds quoted below each equation.

To validate the new relativistic framework we have developed a rigorous development and testing plan with GipsyX [20]. GipsyX is precision software developed by JPL for GNSS-based positioning, navigation, timing, and Earth science applications. It supports GPS, GLONASS, BeiDou, and Galileo systems and offers precise, centimeter-level

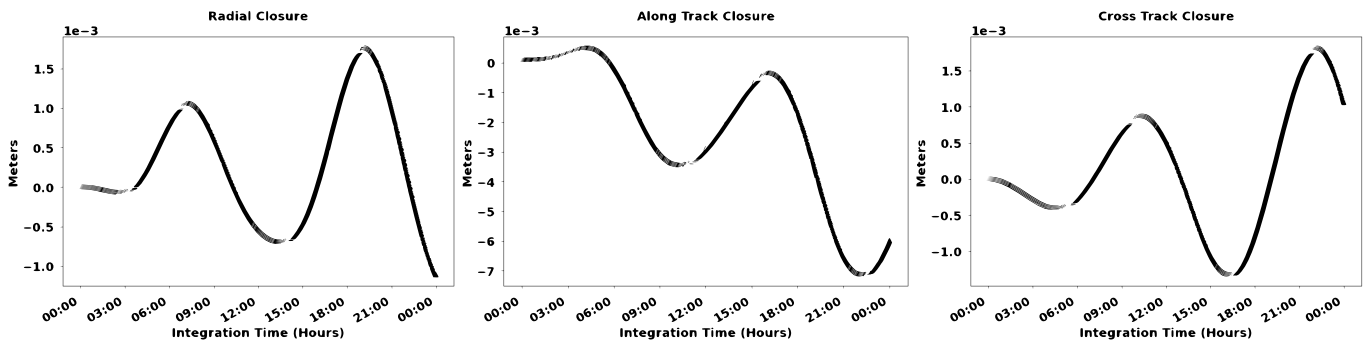


FIG. 1. Millimeter-level closure test of the BCRS implementation with JPL GipsyX. Panels show radial/along-track/cross-track closure residuals in meters (note the 10^{-3} scale, i.e., millimeter range) versus integration time (hours).

TABLE V. Configuration used for the closure test shown in Fig. 1.

Item	Value
Ephemeris	JPL DE440 (argument: TDB) [4]
Earth gravity	Spherical harmonics to degree/order $N = M = 20$ (TT-compatible)
Third bodies	Sun and Moon tidal terms (Newtonian)
Relativity (GCRS)	Schwarzschild, de Sitter, Lense-Thirring per Eq. (78)
Relativity (BCRS)	EIH point-mass terms per Eq. (63)
SRP/tides	Standard GipsyX models (identical in both frames)
Span	24 h; start epoch UTC: 2025-01-01 00:00:00
Transformations	Full vs. screened: Eqs. (36) [position], (42) [velocity], (51) [acceleration]

positioning for various platforms, including low-Earth orbiters and terrestrial stations. GipsyX integrates real-time and post-processing capabilities and is continuously updated to meet the evolving demands of space geodesy.³

We have undertaken a comprehensive implementation approach to enhance the accuracy of GNSS positioning by incorporating advanced computational models:

- Imported and used the JPL planetary ephemeris DE440 [4] for high-precision celestial mechanics.
- Implemented the BCRS, integrating state-of-the-art relativistic models to ensure precise trajectory computations.
- Developed multiple centers of integration to facilitate robust data handling and computational efficiency.
- Integrated models for lunar orientation, lunar gravity, and lunar albedo to enhance lunar navigation capabilities.

To validate the implementation of the barycentric coordinate reference frame and the associated transformations, we conducted a series of rigorous tests:

1. Integrated a GPS orbit within the GCRS to establish a baseline for comparison.
2. Transformed the orbital state from the GCRS to the BCRS, while maintaining high accuracy in the transformation process.
3. Re-integrated the GPS orbit in the BCRS, starting from the initial condition transformed from the GCRS.
4. Compared the integrated orbit in the BCRS (from Step 3) with the transformed orbit in the GCRS (from Step 2) to assess the precision and accuracy of the transformations.

This testing procedure ensures that the implemented models and transformations meet the requirements for millimeter-level consistency in GNSS-enabled spacecraft navigation.

The numerical analysis conducted between the GCRS and the BCRS demonstrates that orbit states and observables can be precisely aligned, provided that the appropriate space-time transformations and relativistic corrections are applied. In the barycentric system, it is crucial not to overlook the relativistic corrections to acceleration. While in

³ For further details on GipsyX, please visit <https://gipsyx.jpl.nasa.gov/>

TABLE VI. Template regression test vectors for $\text{GCRS} \leftrightarrow \text{BCRS}$ transformations.

Item	Input	Output	Notes
Time map	$\text{TT} = \text{TT}(\text{UTC } 2025\text{-}01\text{-}01 \text{ } 00\text{:}00\text{:}00)$	$\text{TDB} = \text{TT} + 1.3 \times 10^{-3} \text{ s} + \text{periodic}$	Eq. (14)
Station pos	$\mathbf{X}_{\text{TT}} = (0, 6\,378\,137, 0) \text{ m}$	$(\mathbf{r}_{\text{E}})_{\text{TDB}} = \mathbf{X}_{\text{TT}} - \Delta\mathbf{X}$	Eq. (36)
MEO state	$(\mathbf{X}, \dot{\mathbf{X}})$ at GPS altitude	$(\mathbf{r}_{\text{E}}, \dot{\mathbf{r}}_{\text{E}})_{\text{TDB}}$	Eqs. (42),(51)

the Earth-centric system, these relativistic corrections to acceleration are less critical, the necessity for space-time transformations for conversion to and from the BCRS remains significant.

The frame-closure residuals defined in Eq. (82) compare the BCRS state obtained by direct integration in the BCRS to the BCRS state obtained by integrating in the GCRS and transforming the resulting state at the same epoch. For the configuration in Table V, the residuals remain in the millimeter regime over the 24 h test interval (Fig. 1), with the largest excursion occurring in the along-track component (peak-to-peak ~ 7 mm).

IV. CONCLUSIONS AND NEXT STEPS

We conducted a comprehensive analysis of general relativistic effects on the dynamics of near-Earth satellites within the GCRS and BCRS frameworks. Our results demonstrate that, when full relativistic corrections are applied, both reference systems yield consistent and equivalent results, enabling high-precision satellite navigation. To keep relativistic modeling biases below the sub-cm level in range-equivalent units and below the $\mathcal{O}(10)$ ps level in one-way time transfer, it is necessary to apply the $\text{TT} \leftrightarrow \text{TDB}$ and $\text{GCRS} \leftrightarrow \text{BCRS}$ transformations consistently with the dynamical and signal-propagation models, which are especially critical for long-duration and deep-space missions. In this paper we validated internal consistency via mm-level 24 h $\text{GCRS} \leftrightarrow \text{BCRS}$ frame closure (Fig. 1), while end-to-end orbit/clock estimation performance additionally depends on the measurement model, data quality, and estimation strategy.

Upcoming cislunar missions will require a formally defined Moon-centered reference system and associated time scales, e.g., [34, 35, 52–54]. Appendix A 1 defines an LCRS coordinate time TCL (Luni-centric coordinate time, in analogy to TCG) together with a scaled lunar-surface time TL (in analogy to TT); both are related to TCB/TDB via the same 1PN transformation structure, see e.g., [8, 21]. A future step toward operational realization is to specify the conventional origin and scaling needed for timekeeping across surface and orbital assets (i.e., a realized coordinated lunar time for clocks), and to validate the $\text{BCRS} \leftrightarrow \text{LCRS}$ chain via dedicated cislunar time-transfer and tracking experiments.

Several of the necessary transformations, particularly between the GCRS and BCRS, have already been implemented in the JPL programs used to generate planetary and lunar ephemerides [25, 38], including the use of astronomical constants compiled before the GRAIL mission [55]. These systems utilize astronomical constants established prior to the GRAIL mission [55] but will require updates to account for increased accuracy demands. These models were also implemented in the high-precision tools like JPL’s GipsyX software, which provides centimeter-level accuracy in real-time satellite navigation and precise orbit determination. Future systems will need to accommodate relativistic time delays on the order of tens of picoseconds and positional discrepancies on the order of millimeters to ensure accurate navigation and timing, especially in lunar and deep-space environments.

The methodology used to develop and validate the relativistic GNSS navigation framework in GCRS and BCRS can be extended to the LCRS to achieve millimeter-level orbit closure and picosecond-level timing consistency in GipsyX. Looking ahead, we identify three potential pathways to mature the LCRS into a flight-ready capability:

1. *Lunar GNSS Pathfinder Missions:* Integrate a compact GNSS receiver and atomic clock payload (e.g. NASA’s Deep Space Atomic Clock DSAC-II or JPL’s Next-Gen On-Orbit Navigator) aboard a Commercial Lunar Payload Services (CLPS) lander or Lunar Gateway module to measure real-time LCRS time offsets and validate centimeter-scale positioning *in situ*.
2. *Lunar Relay Satellite Demonstrations:* Deploy a smallsat in a halo orbit about the Earth–Moon L2 point, equipped with dual-frequency GNSS antennas synchronized to a space-qualified hydrogen maser. This will exercise the LCRS transformations under large Sun–Moon gravitational gradients and characterize residual frame-bias errors below 1 cm.
3. *Clock-Experiment Campaigns:* Perform precision time-transfer tests between DSAC-class clocks on Earth-orbiting GNSS platforms and LCRS-referenced clocks on lunar orbiters, quantifying relativistic scale factors and assessing long-term stability at the 10^{-17} level using extended relativistic framework (e.g., [21]).

By executing such demonstrations—first in MEO and then in representative Earth–Moon geometries—one can validate the end-to-end $\text{GCRS}/\text{BCRS}/\text{LCRS}$ reference-system infrastructure (state transformations, time scales, and 1PN

light-time) in a mission-relevant configuration. This infrastructure is a prerequisite for cm-class cislunar navigation and ps-level time-transfer; achieved user-level performance will additionally depend on signal availability, measurement quality, and the estimation strategy.

Ongoing work focuses on refining the relativistic corrections and coordinate transformations across GCRS, BCRS, and LCRS, and on integrating them into operational systems such as JPL’s GipsyX. These efforts are essential for upcoming missions targeting the Earth-Moon system and beyond that demand stringent positional accuracy and timing precision. Results, when available, will be reported in subsequent publications.

ACKNOWLEDGMENTS

The work described here was carried out at the Jet Propulsion Laboratory, California Institute of Technology, Pasadena, California, under a contract with the National Aeronautics and Space Administration.

-
- [1] T. D. Moyer, *Formulation for Observed and Computed Values of Deep Space Network Data Types for Navigation*, JPL Deep-Space Communications and Navigation Series (John Wiley & Sons, Inc., Hoboken, New Jersey, 2003).
 - [2] O. Montenbruck and E. Gill, *Satellite Orbits. Models, Methods, and Applications. (3-rd ed.)* (Springer Berlin, Heidelberg, 2005).
 - [3] M. H. Soffel and W.-B. Han, *Applied General Relativity: Theory and Applications in Astronomy, Celestial Mechanics and Metrology* (Springer, Cham, Switzerland, 2019).
 - [4] R. S. Park, W. M. Folkner, J. G. Williams, and D. H. Boggs, The JPL Planetary and Lunar Ephemerides DE440 and DE441, *Astron. J.* **161**, 105 (2021).
 - [5] G. Petit and B. Luzum (eds.), *IERS Technical Note #36* (“IERS Conventions (2010)”, Frankfurt am Main: Verlag des Bundesamts für Kartographie und Geodäsie, 2010. 179 pp., ISBN 3-89888-989-6”, 2010).
 - [6] S. M. Kopeikin, M. Efroimsky, and G. Kaplan, *Relativistic Celestial Mechanics of the Solar System* (Wiley-VCH, Berlin, 2011).
 - [7] M. Soffel, S. A. Klioner, G. Petit, P. Wolf, S. M. Kopeikin, P. Bretagnon, V. A. Brumberg, N. Capitaine, T. Damour, T. Fukushima, B. Guinot, T.-Y. Huang, L. Lindgren, C. Ma, K. Nordtvedt, J. C. Ries, P. K. Seidelmann, D. Vokrouhlický, C. M. Will, and C. Xu, The IAU 2000 Resolutions for Astrometry, Celestial Mechanics, and Metrology in the Relativistic Framework: Explanatory Supplement, *Astron. J.* **126**, 2687 (2003).
 - [8] S. G. Turyshev, J. G. Williams, D. H. Boggs, and R. S. Park, Relativistic Time Transformations between the Solar System Barycenter, Earth, and Moon, *ApJ* **985**, 140 (2025), arXiv:2406.16147 [astro-ph.EP].
 - [9] G. H. Kaplan, The IAU resolutions on astronomical reference systems, time scales, and earth rotation models: explanation and implementation, U.S. Naval Observatory Circulars **179** (2005), arXiv:astro-ph/0602086.
 - [10] S. G. Turyshev, V. T. Toth, and M. V. Sazhin, General relativistic observables of the GRAIL mission, *Phys. Rev. D* **87**, 024020 (2013), arXiv:1212.0232 [gr-qc].
 - [11] S. G. Turyshev, M. V. Sazhin, and V. T. Toth, General relativistic laser interferometric observables of the GRACE-Follow-On mission, *Phys. Rev. D* **89**, 105029 (2014), arXiv:1402.7111 [gr-qc].
 - [12] K. Sošnica, G. Bury, R. Zajdel, K. Kazmierski, J. Ventura-Traveset, R. Prieto-Cerdeira, and L. Mendes, General relativistic effects acting on the orbits of Galileo satellites, *CMDA* **133**, 14 (2021).
 - [13] S. G. Turyshev and V. T. Toth, Spherical harmonics representation of the gravitational phase shift, *Phys. Rev. D* **107**, 104031 (2023), arXiv:2303.07270 [gr-qc].
 - [14] K. Sošnica and F. Gayn, Orbital relativistic correction resulting from the Earth’s oblateness term, *J. Geod.* **99**, 52 (2025).
 - [15] J. F. Zumberge, M. B. Hefflin, D. C. Jefferson, M. M. Watkins, and F. H. Webb, Precise point positioning for the efficient and robust analysis of GPS data from large networks, *JGR: Solid Earth* **102**, 5005 (1997).
 - [16] J. Kouba and P. Héroux, Precise point positioning using IGS orbit and clock products, *GPS Solutions* **5**, 12 (2001).
 - [17] P. J. G. Teunissen and O. Montenbruck, eds., *Springer Handbook of Global Navigation Satellite Systems* (Springer, 2017).
 - [18] B. D. Tapley, B. E. Schutz, and G. H. Born, *Statistical Orbit Determination* (Elsevier Academic Press, 2004).
 - [19] C. W. Misner, K. S. Thorne, and J. A. Wheeler, *Gravitation* (W.H. Freeman and Co., San Francisco, 1973).
 - [20] W. Bertiger, Y. Bar-Sever, A. Dorsey, B. Haines, N. Harvey, D. Hemberger, M. Hefflin, W. Lu, M. Miller, A. W. Moore, D. Murphy, P. Ries, L. Romans, A. Sibois, A. Sibthorpe, B. Szilagyi, M. Vallisneri, and P. Willis, GipsyX/RTGx, a new tool set for space geodetic operations and research, *Adv. Space Res.* **66**, 469 (2020).
 - [21] S. G. Turyshev, *High-Precision Relativistic Time Scales for Cislunar Navigation* (2025), arXiv:2507.22145 [gr-qc].
 - [22] L. D. Landau and E. M. Lifshitz, *The Classical Theory of Fields* (in Russian), 7th ed. (Nauka, Moscow, 1988).
 - [23] R. S. Park, W. M. Folkner, A. S. Konopliv, J. G. Williams, D. E. Smith, and M. T. Zuber, Precession of Mercury’s Perihelion from Ranging to the MESSENGER Spacecraft, *ApJ* **153**, 121 (2017).
 - [24] R. Mecheri and M. Meftah, Updated values of solar gravitational moments j_{2n} using hmi helioseismic inference of internal rotation, *MNRAS* **506**, 2671 (2021).

- [25] J. G. Williams and D. H. Boggs, The JPL Lunar Laser Range Model (2015), JPL Interoffice Memorandum, IOM 335-JGW,DHB-20150701-32.
- [26] B. Guinot, Résolution A4 (1991), Union Astronomique Internationale, sur les systèmes de référencé: échelles de temps., in *Journées 1992: Systèmes de référence spatio-temporels* (1992) pp. 12–21.
- [27] E. Groten, Fundamental Parameters and Current (2004) Best Estimates of the Parameters of Common Relevance to Astronomy, Geodesy, and Geodynamics by Erwin Groten, IPGD, Darmstadt, *J. of Geodesy* **77**, 724 (2004).
- [28] V. A. Brumberg and E. Groten, IAU resolutions on reference systems and time scales in practice, *Astron. Astrophys.* **367**, 1070 (2001).
- [29] IAU, Resolution b.3 (Cambridge University Press, New York, 2009) p. 42, Proc. of the 26th General Assembly (Prague, Czech Republic, 2006).
- [30] E. M. Standish, *JPL Planetary and Lunar Ephemerides, DE405/LE405*, Interoffice Memorandum JPL IOM 312.F-98-048 (Jet Propulsion Laboratory, California Institute of Technology, 1998).
- [31] L. Fairhead and P. Bretagnon, An analytical formula for the time transformation TB-TT., *Astron. Astrophys.* **229**, 240 (1990).
- [32] C. Huang, J. C. Ries, B. D. Tapley, and M. M. Watkins, Relativistic Effects for Near Earth Satellite Orbit Determination, *CMDA* **48**, 167 (1990).
- [33] W. M. Folkner, J. G. Williams, D. H. Boggs, R. S. Park, and P. Kuchynka, *The Planetary and Lunar Ephemerides DE430 and DE431*, The Interplanetary Network Progress Report 42-196 (Jet Propulsion Laboratory, California Institute of Technology, 2014).
- [34] A. Delépaüt, P. Giordano, J. Ventura-Traveset, D. Blonski, M. Schönfeldt, P. Schoonejans, S. Aziz, and R. Walker, Use of GNSS for lunar missions and plans for lunar in-orbit development, *Adv. Space Res.* **66**, 2739 (2020).
- [35] United Nations Office for Outer Space Affairs, *The Interoperable Global Navigation Satellite Systems Space Service Volume*, Tech. Rep. ST/SPACE/75 (United Nations, 2018) date of issue: 2018-10-30.
- [36] C. M. Will, *Theory and Experiment in Gravitational Physics* (Cambridge University Press, Cambridge, UK, 1993).
- [37] S. Kopeikin and I. Vlasov, Parametrized post-Newtonian theory of reference frames, multipolar expansions and equations of motion in the N-body problem, *Phys. Rep.* **400**, 209 (2004).
- [38] E. M. Standish and J. G. Williams, Orbital ephemerides of the sun, moon, and planets, in *Explanatory Supplement to the American Ephemeris and Nautical Almanac*, edited by P. K. Seidelmann (Mill Valley: University Science Books, 2008) Chap. 8.
- [39] A. Hees, S. Bertone, and C. Le Poncin-Lafitte, Relativistic formulation of coordinate light time, Doppler, and astrometric observables up to the second post-Minkowskian order, *Phys. Rev D* **89**, 064045 (2014).
- [40] N. Ashby, Relativity in the Global Positioning System, *LRR* **6**, 1 (2003).
- [41] L. Blanchet, C. Salomon, P. Teyssandier, and P. Wolf, Relativistic theory for time and frequency transfer to order c^{-3} , *Astron. Astrophys.* **370**, 320 (2001).
- [42] M. Abramowitz and I. A. Stegun, *Handbook of Mathematical Functions: with Formulas, Graphs, and Mathematical Tables*. (Dover Publications, New York; revised edition, 1965).
- [43] B. Godard, F. Budnik, T. Morley, and L. A. Lopez, *Relativistic acceleration of planetary orbiters* (2012), Proc. 23rd Intern. Symposium on Space Flight Dynamics, Pasadena, California, Oct. 29 - Nov. 2, 2012.
- [44] V. A. Brumberg and S. M. Kopeikin, Relativistic reference systems and motion of test bodies in the vicinity of the Earth., *Nuovo Cimento, B Serie* **103**, 63 (1989).
- [45] K. Schwarzschild, Über das Gravitationsfeld eines Massenpunktes nach der Einsteinschen Theorie, Sitzungsberichte der Königlich Preussischen Akademie der Wissenschaften , 189 (1916).
- [46] K. Schwarzschild, On the gravitational field of a mass point according to Einstein's theory, *GRG* **35**, 951 (2003).
- [47] J. Lense and H. Thirring, On the influence of the proper rotation of a central body on the motion of the planets and the moon, according to Einstein's theory of gravitation, *Zeit. Phys.* **19**, 156 (1918).
- [48] W. de Sitter, Einstein's theory of gravitation and its astronomical consequences. Third paper, *MNRAS* **78**, 3 (1917).
- [49] T. Damour, M. Soffel, and C. Xu, General-relativistic celestial mechanics. I. Method and definition of reference systems, *Phys. Rev. D* **43**, 3273 (1991).
- [50] S. G. Turyshev and V. T. Toth, New perturbative method for solving the gravitational N-body problem in the general theory of relativity, *Int. J. Mod. Phys. D* **24**, 1550039-141 (2015), arXiv:1304.8122 [gr-qc].
- [51] M. H. Soffel, *Relativity in Astrometry, Celestial Mechanics and Geodesy* (Springer Berlin, Heidelberg, 1989).
- [52] Y. Bar-Sever, E. Burt, K.-M. Cheung, T. Ely, J. Hamkins, S. Lichten, M. Sanchez Net, D. Ogbe, R. Tjoelker, Z. Towfic, and N. Yu, Architectures and Technology Investment Priorities for Positioning, Navigation, and Timing at the Moon and Mars (2024), The Interplanetary Network Progress Report, Volume 42-237, pp. 1-60, May 15, 2024, https://ipnpr.jpl.nasa.gov/progress_report/42-237/42-237A.pdf.
- [53] D. J. Israel, K. D. Mauldin, C. J. Roberts, J. W. Mitchell, A. A. Pulkkinen, L. V. D. Cooper, M. A. Johnson, S. D. Christe, and C. J. Gramling, LunaNet: a flexible and extensible lunar exploration communications and navigation infrastructure, in *Proc. IEEE Aerospace Conference* (Big Sky, MT, USA, 2020) NASA NTRS Document ID: 20200001555.
- [54] J. J. K. Parker, F. Dovis, B. Anderson, L. Ansalone, B. Ashman, F. H. Bauer, G. D'Amore, C. Facchinetti, S. Fantinato, G. Impresario, S. A. McKim, E. Miotti, J. J. Miller, M. Musmeci, O. Pozzobon, L. Schlenker, A. Tuozzi, and L. Valencia, The Lunar GNSS Receiver Experiment (LuGRE), in *Proc. of the International Technical Meeting (ITM) 2022* (Institute of Navigation, Long Beach, CA, USA, 2022) NASA NTRS Document ID: 20220002074.

- [55] R. B. Roncoli, [Lunar Constants and Models Document](#) (2005), Lunar Constants and Models Document. JPL Technical Document D-32296.
- [56] International Astronomical Union, [Resolution II: to establish a standard lunar celestial reference system \(LCRS\) and lunar coordinate time \(TCL\)](#), IAU XXXII General Assembly (Cape Town), Resolution document dated 15 April 2024 (2024).
- [57] B. A. Archinal, C. H. Acton, M. F. A’Hearn, *et al.*, Report of the IAU Working Group on Cartographic Coordinates and Rotational Elements: 2015, [CMDA 130, 22](#) (2018).
- [58] D. E. Smith, M. T. Zuber, G. A. Neumann, E. Mazarico, F. G. Lemoine, I. Head, James W., P. G. Lucey, O. Aharonson, M. S. Robinson, X. Sun, M. H. Torrence, M. K. Barker, J. Oberst, T. C. Duxbury, D. Mao, O. S. Barnouin, K. Jha, D. D. Rowlands, S. Goossens, D. Baker, S. Bauer, P. Gläser, M. Lemelin, M. Rosenburg, M. M. Sori, J. Whitten, and T. Mcclanahan, Summary of the results from the lunar orbiter laser altimeter after seven years in lunar orbit, [Icarus 283, 70](#) (2017).
- [59] J. G. Williams, A. S. Konopliv, D. H. Boggs, R. S. Park, D.-N. Yuan, F. G. Lemoine, S. Goossens, E. Mazarico, F. Nimmo, R. C. Weber, S. W. Asmar, H. J. Melosh, G. A. Neumann, R. J. Phillips, D. E. Smith, S. C. Solomon, M. M. Watkins, M. A. Wieczorek, J. C. Andrews-Hanna, J. W. Head, W. S. Kiefer, I. Matsuyama, P. J. McGovern, G. J. Taylor, and M. T. Zuber, Lunar interior properties from the GRAIL mission, [JGR: Planets 119, 1546](#) (2014).
- [60] A. S. Konopliv, R. S. Park, D.-N. Yuan, S. W. Asmar, M. M. Watkins, J. G. Williams, E. Fahnestock, G. Kruizinga, M. Paik, D. Strelakov, N. Harvey, D. E. Smith, and M. T. Zuber, The JPL lunar gravity field to spherical harmonic degree 660 from the GRAIL Primary Mission, [JGR: Planets 118, 1415](#) (2013).
- [61] X. Lu, T.-N. Yang, and Y. Xie, Lunar time ephemeris LTE440: Definitions, algorithm, and performance, [Astron. Astrophys. 704, A76](#) (2025).
- [62] Z. Martinec and K. Pec, A Determination of the Parameters of the Level Surface of Lunar Gravity, [Earth, Moon, and Planets 43, 21](#) (1988).

Appendix A: Coordinate Transformation for the Moon System

1. Introducing the LCRS

The International Astronomical Union has adopted a standard Lunar Celestial Reference System (LCRS) and Lunar Coordinate Time (TCL) [56]. In this work, we follow that framework and the detailed development in [21] to provide implementation-ready coordinate and time transformations between the BCRS and the LCRS. The LCRS is realized as a kinematically non-rotating reference system centered at the Moon and aligned with the ICRS axes, analogous to the relation between the BCRS and the GCRS. The realization of lunar body-fixed orientation and cartographic elements follows the IAU Working Group recommendations; see, e.g., [57]. These conventions enter the LCRS through the adopted lunar rotation model and the definition of surface site coordinates.

Following the structure of the GCRS metric [21], the LCRS with coordinates $(\mathcal{T} = \text{TCL}, \boldsymbol{\mathcal{X}})$ is described by a metric of similar form. The components of this metric are tailored to account for the Moon’s gravitational field, tidal effects from nearby massive bodies, and the relativistic corrections required for high-precision trajectory modeling can be expressed in the form (see details in [8]):

$$ds_{\text{LCRS}}^2 = \left\{ 1 - 2c^{-2} \left(U_{\text{M}}(\mathcal{T}, \boldsymbol{\mathcal{X}}) + U_{\text{tid}}^*(\mathcal{T}, \boldsymbol{\mathcal{X}}) \right) + \mathcal{O}(c^{-4}) \right\} c^2 d\mathcal{T}^2 - \left\{ 1 + 2c^{-2} \left(U_{\text{M}}(\mathcal{T}, \boldsymbol{\mathcal{X}}) + U_{\text{tid}}^*(\mathcal{T}, \boldsymbol{\mathcal{X}}) \right) + \mathcal{O}(c^{-4}) \right\} d\boldsymbol{\mathcal{X}}^2, \quad (\text{A1})$$

where $U_{\text{M}}(\mathcal{T}, \boldsymbol{\mathcal{X}})$ represents the Newtonian gravitational potential of the isolated Moon, and $U_{\text{tid}}^*(\mathcal{T}, \boldsymbol{\mathcal{X}})$ denotes the tidal potential generated by all other solar system bodies (excluding the Moon), both evaluated at the origin of the LCRS. The omitted terms, arising from U_{M}^2 , may contribute up to $\simeq 8.43 \times 10^{-19}$, which is negligible for our purposes.

Analogous to the coordinate transformations between GCRS and BCRS described earlier, the time and position transformations between the LCRS $(\mathcal{T} = \text{TCL}, \boldsymbol{\mathcal{X}})$ and the BCRS $(t = \text{TCB}, \mathbf{x})$ can be expressed as follows:

$$\mathcal{T} = t - c^{-2} \left\{ \int_{t_0}^t \left(\frac{1}{2} v_{\text{M}}^2 + \sum_{\text{B} \neq \text{M}} \frac{GM_{\text{B}}}{r_{\text{BM}}} \right) dt + (\mathbf{v}_{\text{M}} \cdot \mathbf{r}_{\text{M}}) \right\} + \mathcal{O}(1.10 \times 10^{-16})(t - t_0), \quad (\text{A2})$$

$$\boldsymbol{\mathcal{X}} = \left(1 + c^{-2} \sum_{\text{B} \neq \text{M}} \frac{GM_{\text{B}}}{r_{\text{BM}}} \right) \mathbf{r}_{\text{M}} + c^{-2} \left\{ \frac{1}{2} (\mathbf{v}_{\text{M}} \cdot \mathbf{r}_{\text{M}}) \mathbf{v}_{\text{M}} + (\mathbf{a}_{\text{M}} \cdot \mathbf{r}_{\text{M}}) \mathbf{r}_{\text{M}} - \frac{1}{2} r_{\text{M}}^2 \mathbf{a}_{\text{M}} \right\} + \mathcal{O}(1.28 \times 10^{-12} \text{ m}), \quad (\text{A3})$$

where $\mathbf{r}_{\text{M}} \equiv \mathbf{x} - \mathbf{x}_{\text{M}}(t)$ with \mathbf{x}_{M} and $\mathbf{v}_{\text{M}} = d\mathbf{x}_{\text{M}}/dt$ being the Moon’s position and velocity vectors in the BCRS. The uncertainty in (A2) is determined by the magnitude of the c^{-4} -term omitted in (A2) that behaves as $\sim c^{-4} \left\{ -\frac{1}{8} v_{\text{M}}^2 - \frac{3}{2} v_{\text{M}}^2 GM_{\text{S}}/r_{\text{M}} + \frac{1}{2} (GM_{\text{S}}/r_{\text{M}})^2 \right\} \lesssim -1.22 \times 10^{-16} = -10.50 \text{ ps/d}$, which was omitted. The uncertainty in (A3) is set by the omitted contribution from the solar quadrupole moment. The inverse transformations to (A2)–(A3) are obtained by moving the c^{-2} -terms on the other side of the equations with appropriate sign changes.

Using (A1) and (A2)–(A3), we will derive the new relativistic time scales applicable to the Moon.

2. Transformation between TL and TDB

Analogous to (7), the time transformation from Lunar Time (TL) at the Moon's surface to Luni-centric Coordinate Time (TCL) involves a change in the rate of time (see nomenclature discussion in [8])

$$\frac{dTCL}{dT_L} = \frac{1}{1 - L_L} = 1 + \frac{L_L}{1 - L_L} \quad \text{or} \quad \frac{dT_L}{dTCL} = 1 - L_L. \quad (\text{A4})$$

For the Moon, constant L_L is derived from its gravity and rotational dynamics as below (see discussion in [21])

$$L_L = \frac{1}{c^2} \left\{ \frac{GM_M}{R_{MQ}} \left(1 + \frac{1}{2} J_{2M} \right) + \frac{1}{2} R_{MQ}^2 \omega_M^2 \right\} + \mathcal{O}(3.27 \times 10^{-15}). \quad (\text{A5})$$

The adopted lunar reference radius for gravity is $R_{MQ} = 1738.0$ km, which is larger than the mean radius of $R_M = 1737.1513$ km [58]. The lunar gravitational constant $GM_M = 4902.800118$ km³/s² (DE440, [4]), and the gravity harmonic J_{2M} is 2.033×10^{-4} [59], with a rotational angular velocity $\omega_M = 2\pi/(27.32166 \text{ d} \times 86400 \text{ s/d}) = 2.6616996 \times 10^{-6} \text{ s}^{-1}$. The corresponding value of L_L , with the larger radius R_{MQ} , is estimated to be $L_L = 3.1390541 \times 10^{-11} \simeq 2.7121 \mu\text{s/d}$. The error bound in (A5) is determined by the omitted term involving the tesseral harmonics $C_{22} = 3.4673798 \times 10^{-5} \pm 1.7 \times 10^{-9}$ of the Moon's gravitational field [60].

The constant L_L allows for the scaling of coordinates and mass parameters to maintain the invariance of the speed of light and the equations of motion within the LCRS during the transformation from TCL to TL. Thus, rather than using the coordinate time $\mathcal{T} = \text{TCL}$, spatial coordinates \mathcal{X} , and mass factors $(GM)_{\text{TCL}}$ associated with the LCRS, we will apply the following scaling for the relevant quantities on the lunar surface:

$$\text{TL} = \text{TCL} - L_L(\text{TCL} - \text{T}_{L0}), \quad \mathcal{X}_{\text{TL}} = (1 - L_L)\mathcal{X}_{\text{TCL}}, \quad (GM)_{\text{TL}} = (1 - L_L)(GM)_{\text{TCL}}, \quad (\text{A6})$$

where T_{L0} is the initial lunar time, which we will leave unspecified for the time being.

The transformation from TCL to TCB is determined using (A2):

$$\text{TCB} - \text{TCL} = \left\{ \frac{1}{c^2} \int \left(\frac{1}{2} v_M^2 + \sum_{B \neq M} \frac{GM_B}{r_{BM}} \right) dt + \frac{1}{c^2} (\mathbf{v}_M \cdot \mathbf{r}_{SM}) \right\}_{\text{TCB}} + \mathcal{O}(c^{-4}), \quad (\text{A7})$$

where \mathbf{v}_M denotes the solar system barycentric velocity vector of the Moon, v_M is its scalar magnitude, U_M represents the external potential at the Moon's center, and \mathbf{r}_{SM} is the vector from the Moon's center to the surface location. The integral is taken from 0 to T . Both potential and kinetic energies are computed in the Moon-centered reference frame. The dot product reaches an annual maximum of $\pm 0.58 \mu\text{s}$, with smaller variations of ± 21 ps occurring at the Moon's sidereal period of 27.32166 d.

Eq. (A7) provides the mean rate between TCL and TCB as follows:

$$\left\langle \frac{dTCL}{dT_{\text{TCB}}} \right\rangle = 1 - L_H, \quad (\text{A8})$$

with L_H estimated to be $L_H = 1.4825362 \times 10^{-8}$, where $\langle \dots \rangle$ denote the long-time averaging, see [8]. Numerical realizations of the (TCL–TCB)/TDB relations consistent with the IAU definition are now available as lunar time ephemerides (e.g., LTE440 [61]), which can be used as an independent validation of the constants and periodic terms entering (A7).

To express TCB via TL, we introduce a constant L_M , which defines the rate between TL and TCB. In analogy with the introduction of L_B , constant L_M can be formally introduced as follows

$$\left\langle \frac{dT_L}{dT_{\text{TCB}}} \right\rangle = 1 - L_M. \quad (\text{A9})$$

Then, by using the chain of time derivatives, we can establish the relationships between the constants L_M , L_L and L_H , similar to (10). Following this approach, and with the use of (A4), (A8) and (A9), we obtain the following:

$$\left\langle \frac{dT_L}{dT_{\text{TCB}}} \right\rangle = \left(\frac{dT_L}{dTCL} \right) \left\langle \frac{dTCL}{dT_{\text{TCB}}} \right\rangle \quad \Rightarrow \quad (1 - L_M) = (1 - L_L)(1 - L_H), \quad (\text{A10})$$

from this, the constant L_M is determined as $L_M \simeq L_L + L_H - L_L L_H = 1.485675294 \times 10^{-8} \approx 1.28362 \text{ ms/d}$.

To develop the (TCB – TL) transformation, we apply (A4), (A10), and (A7), leading to the following result:

$$\text{TCB} - \text{TL} = \frac{L_L}{1 - L_L} (\text{TL} - \text{T}_{L0}) + \frac{1}{1 - L_M} \left\{ \frac{1}{c^2} \int_{\text{T}_{L0}}^{\text{TL}} \left(\frac{1}{2} v_M^2 + \sum_{B \neq M} \frac{GM_B}{r_{BM}} \right) dt + \frac{1}{c^2} (\mathbf{v}_M \cdot \mathbf{r}_{OM}) \right\}_{\text{TL}}, \quad (\text{A11})$$

where \mathbf{r}_{0M} is the position vector of a specific site on the lunar surface in the LCRS.

Expression (A11) allows us to formulate (TDB – TL) as a function of TL. To achieve this, we use (11), (A10), and (A11), to express TDB – TL as a function of TL as shown below

$$\begin{aligned} \text{TDB} - \text{TL} &= \text{TDB}_0 - \frac{L_B - L_L}{1 - L_L} (\text{TL} - \text{T}_0) + L_B (\text{T}_0 - \text{T}_{L0}) + \\ &+ \frac{1 - L_B}{1 - L_M} \left\{ \frac{1}{c^2} \int_{\text{T}_{L0}}^{\text{TL}} \left(\frac{1}{2} v_M^2 + \sum_{B \neq M} \frac{GM_B}{r_{BM}} \right) d\text{TL} + \frac{1}{c^2} (\mathbf{v}_M \cdot \mathbf{r}_{0M\text{TL}}) \right\} + \mathcal{O}(c^{-4}). \end{aligned} \quad (\text{A12})$$

It is useful to express the difference (TDB – TL) as a function of TDB. This can be achieved by applying (11), (A6), (A7), and (A10), resulting in the following expression (see details in [8, 21]):

$$\begin{aligned} \text{TDB} - \text{TL} &= \frac{1 - L_L}{1 - L_B} \text{TDB}_0 - \frac{L_B - L_L}{1 - L_B} (\text{TDB} - \text{T}_0) + L_L (\text{T}_0 - \text{T}_{L0}) + \\ &+ \frac{1 - L_L}{1 - L_B} \left\{ \frac{1}{c^2} \int_{\text{T}_0 + \text{TDB}_0}^{\text{TDB}} \left(\frac{1}{2} v_M^2 + \sum_{B \neq M} \frac{GM_B}{r_{BM}} \right) d\text{TDB} + \frac{1}{c^2} (\mathbf{v}_M \cdot \mathbf{r}_{0M\text{TDB}}) \right\} + \mathcal{O}(c^{-4}). \end{aligned} \quad (\text{A13})$$

3. Relationships between TL and TT

Using expression (12) together with (A13) and considering the Moon-related terms, it is instructive to express the BCRS position vector between a body B and the Moon as $\mathbf{r}_{BM} = \mathbf{r}_{BE} + \mathbf{r}_{EM}$, where $\mathbf{r}_{BE} = \mathbf{x}_E - \mathbf{x}_B$ is the position vector from the body B to the Earth, and $\mathbf{r}_{EM} = \mathbf{x}_M - \mathbf{x}_E$ is the Earth-Moon relative position vector, also $r_{BM} \equiv |\mathbf{x}_{BM}|$, $r_{EM} \equiv |\mathbf{x}_{EM}|$. Also, by representing $\mathbf{v}_M = \mathbf{v}_E + \mathbf{v}_{EM}$, where \mathbf{v}_E is the BCRS velocity of the Earth and \mathbf{v}_{EM} is the Earth-Moon relative velocity, we present expression (TL – TT) as a function of TT in the following form [8, 21]

$$\begin{aligned} \text{TL} - \text{TT} &= \frac{L_G - L_L}{1 - L_B} (\text{TT} - \text{T}_0) - L_L (\text{T}_0 - \text{T}_{L0}) - \\ &- \frac{1}{c^2} \int_{\text{T}_0}^{\text{TT}} \left\{ \frac{1}{2} v_{EM}^2 + \frac{GM_E - 2GM_M}{r_{EM}} + W_{EM}^S \right\} d\text{TT} - \frac{1}{c^2} (\mathbf{v}_{EM} \cdot \boldsymbol{\mathcal{X}}_{\text{TT}}) + \mathcal{O}(c^{-5}; 4.76 \times 10^{-19} (\text{TT} - \text{TT}_0)), \end{aligned} \quad (\text{A14})$$

where the solar tidal potential at the Moon W_{EM}^S is given by

$$W_{EM}^S = \sum_{\ell=2}^3 \frac{GM_S}{r_{SE}} \left(\frac{r_{EM}}{r_{SE}} \right)^\ell P_\ell(\mathbf{n}_{SE} \cdot \mathbf{n}_{EM}) + \mathcal{O}(4.30 \times 10^{-19}), \quad (\text{A15})$$

where we kept the solar octupole tidal term $\ell = 3$. The magnitude of this term was estimated to be $\simeq 1.68 \times 10^{-16}$, which is small, but large enough to be part of the model. The error bound here is set by the solar $\ell = 4$ tidal contribution, evaluated to be $c^{-2} GM_S / r_{SE} (r_{EM} / r_{SE})^4 \simeq 4.30 \times 10^{-19}$.

We can present result (A14) in a different form by introducing the constant L_{EM} and periodic terms P_{EM} as below

$$\frac{1}{c^2} \left\{ \frac{1}{2} v_{EM}^2 + \frac{GM_E - 2GM_M}{r_{EM}} + W_{EM}^S \right\} = L_{EM} + \dot{P}_{EM}(t) + \mathcal{O}(c^{-5}; 4.76 \times 10^{-19}), \quad (\text{A16})$$

where the constant rate $L_{EM} \simeq L_H - L_C$ and the periodic terms $\dot{P}_{EM}(t) \simeq \dot{P}_H(t) - \dot{P}(t)$ are given as below:

$$L_{EM} = \frac{1}{c^2} \left\{ \left\langle \frac{1}{2} v_{EM}^2 + \frac{GM_E - 2GM_M}{r_{EM}} \right\rangle + \langle W_{EM}^S \rangle \right\}, \quad (\text{A17})$$

$$\dot{P}_{EM}(t) = \frac{1}{c^2} \left\{ \frac{1}{2} v_{EM}^2 + \frac{GM_E - 2GM_M}{r_{EM}} - \left\langle \frac{1}{2} v_{EM}^2 + \frac{GM_E - 2GM_M}{r_{EM}} \right\rangle + W_{EM}^S - \langle W_{EM}^S \rangle \right\}. \quad (\text{A18})$$

Result (A16), together with (A17) and (A18), provides valuable insight into the structure of the constant term L_{EM} and the periodic terms $P_{EM}(t)$. These expressions can be used to explicitly establish the structure of the series $P_{EM}(t)$.

Finally, using (A16) in (A14), we express (TL – TT) as a function of TT:

$$\begin{aligned} \text{TL} - \text{TT} &= \frac{L_G - L_L - L_{EM}}{1 - L_B} (\text{TT} - \text{T}_0) - L_L (\text{T}_0 - \text{T}_{L0}) - \left(P_{EM}(\text{TT}) - P_{EM}(\text{T}_0) \right) - \frac{1}{c^2} (\mathbf{v}_{EM} \cdot \boldsymbol{\mathcal{X}}_{\text{TT}}) + \\ &+ \mathcal{O}(4.76 \times 10^{-19} (\text{TT} - \text{T}_0)), \end{aligned} \quad (\text{A19})$$

where \mathcal{X}_{TT} is the TT-compatible lunicentric position of the lunar clock.

Considering the $O(c^{-2})$ term in L_{EM} (A17), we use Moon–Earth relative speed of $v_{\text{EM}} \approx 1022$ m/s, so the kinematic dilation contributes $c^{-2} \langle \frac{1}{2} v_{\text{EM}}^2 \rangle \simeq 5.81 \times 10^{-12}$, well above our 5×10^{-18} cutoff. Taking r_{EM} to be the instantaneous Earth–Moon separation, the Newtonian monopole term at the Earth–Moon distance was estimated to contribute up to $c^{-2} (GM_{\text{E}} - 2GM_{\text{M}})/r_{\text{EM}} \simeq 1.13 \times 10^{-11}$. The solar quadrupole tide W_{EM}^{S} yields $c^{-2} \langle W_{\text{EM}}^{\text{S}} \rangle \simeq c^{-2} \frac{1}{4} GM_{\text{S}} r_{\text{EM}}^2 / r_{\text{SE}}^3 \simeq 1.63 \times 10^{-14}$. As a result, collecting all the contributions, the secular-drift coefficient for the Earth–Moon system is

$$L_{\text{EM}} = 1.709\,390\,6 \times 10^{-11} = 1.4769 \mu\text{s/d}. \quad (\text{A20})$$

With $L_{\text{EM}} \simeq L_{\text{H}} - L_{\text{C}} = 1.4769 \mu\text{s/d}$, the total constant rate between the clock on or near the lunar surface and its terrestrial analogue to the accepted level of accuracy is estimated to be

$$L_{\text{B}} - L_{\text{M}} \simeq L_{\text{G}} - L_{\text{L}} - L_{\text{EM}} = (60.2146 - 2.7121 - 1.4769) \mu\text{s/d} = 56.0256 \mu\text{s/d}. \quad (\text{A21})$$

Note that, if the smaller value for the lunar radius R_{M} is used in (A5) instead of R_{Mq} , the value of L_{L} is estimated to be $L_{\text{L}} = 3.140\,587\,7 \times 10^{-11} \simeq 2.7135 \mu\text{s/d}$. With this value, the total rate in (A21) is $L_{\text{B}} - L_{\text{M}} = 56.0242 \mu\text{s/d}$. Also, if the selenoid value of $W_{\text{EM}} = 2821713.3 \text{ m}^2\text{s}^{-2}$ from [62] is used to determine $L_{\text{L}} = 3.139\,579\,5 \times 10^{-11} \simeq 2.7126 \mu\text{s/d}$, the value of $L_{\text{B}} - L_{\text{M}} = 56.0251 \mu\text{s/d}$. This dispersion highlights the need for further studies of the lunar constants.

Now we consider the periodic term P_{EM} , see (A18). From the vis–viva relation for the Moon’s motion about the Earth–Moon barycenter given as $v_{\text{EM}}^2(r) = (GM_{\text{E}} + GM_{\text{M}})(2/r_{\text{EM}} - 1/a_{\text{EM}})$, with $r_{\text{EM}} = a_{\text{EM}}(1 - e_{\text{M}} \cos E)$, with $e_{\text{M}} = 0.0549$ being the Moon’s orbital eccentricity. With these quantities, the orbital part of integrand in (A16) reads

$$\frac{1}{c^2} \left\{ \frac{1}{2} v_{\text{EM}}^2 + \frac{GM_{\text{E}} - 2GM_{\text{M}}}{r_{\text{EM}}} \right\} = \frac{1}{c^2} \left\{ \frac{2GM_{\text{E}} - GM_{\text{M}}}{r_{\text{EM}}} - \frac{GM_{\text{E}} + GM_{\text{M}}}{2a_{\text{EM}}} \right\}.$$

Using this result in (A18) and expanding r_{EM} to first order in e_{M} , we can write $r_{\text{EM}} = a_{\text{EM}}(1 - e_{\text{M}} \cos[\omega_{\text{M}}(t - t_0)] + \mathcal{O}(e_{\text{M}}^2))$, where ω_{M} is the Moon’s mean orbital angular rate, we have [8, 21]

$$\begin{aligned} \delta \dot{P}_{\text{EM}}(t) &= \frac{1}{c^2} \left\{ \frac{1}{2} v_{\text{EM}}^2 + \frac{GM_{\text{E}} - 2GM_{\text{M}}}{r_{\text{EM}}} - \left\langle \frac{1}{2} v_{\text{EM}}^2 + \frac{GM_{\text{E}} - 2GM_{\text{M}}}{r_{\text{EM}}} \right\rangle \right\} = \\ &= \frac{1}{c^2} (2GM_{\text{E}} - GM_{\text{M}}) \left(\frac{1}{r_{\text{EM}}} - \frac{1}{a_{\text{EM}}} \right) \simeq \frac{1}{c^2} (2GM_{\text{E}} - GM_{\text{M}}) \frac{e_{\text{M}}}{a_{\text{EM}}} \cos[\omega_{\text{M}}(t - t_0)] = \\ &= 1.259\,047 \times 10^{-12} \cos[\omega_{\text{M}}(t - t_0)] = 0.109 \cos[\omega_{\text{M}}(t - t_0)] \mu\text{s/d}. \end{aligned} \quad (\text{A22})$$

Integrating this result in time gives

$$\delta P_{\text{EM}}(t) \simeq -\frac{1}{c^2} (2GM_{\text{E}} - GM_{\text{M}}) \frac{e_{\text{M}}}{a_{\text{EM}} \omega_{\text{M}}} \sin[\omega_{\text{M}}(t - t_0)] = -0.473 \sin[\omega_{\text{M}}(t - t_0)] \mu\text{s}. \quad (\text{A23})$$

Thus, as shown in (A21), there is a secular trend between a clock on the surface of the Moon and one on the Earth’s surface. This trend occurs at a rate of $(L_{\text{B}} - L_{\text{M}})/(1 - L_{\text{B}}) = 6.484\,440\,4 \times 10^{-10} = 56.0256 \mu\text{s/d}$, with the lunar clock running faster than its terrestrial counterpart. Additionally, there are periodic terms represented by the series $P_{\text{EM}}(t)$ with the largest contribution of $0.473 \sin[\omega_{\text{M}}(t - t_0)] \mu\text{s}$, as given by (A23) with many smaller terms with various periods [21]. Lastly, small site-dependent terms also contribute at specific periods [8].

4. Position transformations

To develop the position transformation for the Moon, we define \mathcal{X}_{TCL} as the position vector of a site on the lunar surface in the LCRS and \mathbf{r}_{M} as the corresponding vector observed from the BCRS (denoted \mathbf{r}_{MTCB}). The goal is to express the relationship between \mathcal{X}_{TCL} and \mathbf{r}_{MTCB} in terms of the TL and TDB timescales. To achieve this, we use (A6) to express the \mathcal{X}_{TCL} via TL and (11) to relate \mathbf{r}_{MTCB} to \mathbf{r}_{MTDB} . This process leads to the following result:

$$\mathcal{X}_{\text{TL}} = \left(1 + L_{\text{B}} - L_{\text{L}} + c^{-2} \sum_{\text{B} \neq \text{M}} \frac{GM_{\text{B}}}{r_{\text{BM}}} \right) \mathbf{r}_{\text{MTDB}} + c^{-2} \left\{ \frac{1}{2} (\mathbf{v}_{\text{M}} \cdot \mathbf{r}_{\text{M}}) \mathbf{v}_{\text{M}} \right\}_{\text{TDB}} + \mathcal{O}(1.00 \times 10^{-7} \text{ m}), \quad (\text{A24})$$

where $\mathbf{r}_{\text{M}} \equiv \mathbf{x} - \mathbf{x}_{\text{M}}(t)$ and similar to (A3), the error is determined by the omitted acceleration-dependent terms. The inverse transformation to that in (A24) is straightforward; it is performed by shifting the c^{-2} -terms to the other side of the equation with the opposite signs. Note that the two leading corrections—the $c^{-2} \sum_{\text{B} \neq \text{M}} GM_{\text{B}}/r_{\text{BM}}$ scale term and the $\frac{1}{2} c^{-2} (\mathbf{v}_{\text{M}} \cdot \mathbf{r}_{\text{M}}) \mathbf{v}_{\text{M}}$ Lorentz term—mirror their Earth analogues in (2).

The first group of terms in (A24) represents a scale change. With $L_B - L_L = 1.547\,380\,65 \times 10^{-8} \approx 1.336\,94$ ms/d and $c^{-2} \langle \sum_{B \neq M} GM_B / r_{BM} \rangle = 0.988438 \times 10^{-8}$, the total is 2.53582×10^{-8} , corresponding to a scale change of 4.41 cm for the Moon's radius. The annual variation is $\pm 1.65 \times 10^{-10}$, or ± 0.29 mm. Additionally, the Earth's and Moon's annual variations will affect the surface-to-surface distance along the center-to-center line, resulting in an annual variation of $1.34 \text{ mm} |\cos l'|$.

The last term in (A24) accounts for the Lorentz contraction. For a site on the Moon's surface, this contraction amounts to 8.7 mm. In the direction of motion, the combined effect of the scale change and Lorentz contraction totals 53 mm, while perpendicular to the motion, the scale change is 44 mm. These adjustments are essential for accurately determining the positions of retroreflectors used in lunar laser ranging (LLR), see [25].

5. Expressions to transform position, velocity and acceleration

Based on the analysis above and considering realistic measurement uncertainties, we use the magnitudes of the terms for a low-lunar-orbit (LLO) orbiter as the basis of our recommendation. Using the same approach as in Sec. II C, we present the expressions recommended for position, velocity, and acceleration transformations for the LCRS⁴:

$$(\mathbf{x} - \mathbf{x}_M)_{\text{TDB}} = \boldsymbol{\mathcal{X}}_{\text{TL}} - (L_B - L_L)\boldsymbol{\mathcal{X}}_{\text{TL}} - c^{-2} \left\{ \frac{1}{2}(\mathbf{v}_M \cdot \boldsymbol{\mathcal{X}})\mathbf{v}_M + \gamma U_{M,\text{ext}} \boldsymbol{\mathcal{X}} \right\}_{\text{TL}} + \mathcal{O}(3.34 \times 10^{-7} \text{ m}), \quad (\text{A25})$$

$$(\dot{\mathbf{x}} - \dot{\mathbf{x}}_M)_{\text{TDB}} = \dot{\boldsymbol{\mathcal{X}}}_{\text{TL}} - c^{-2} \left\{ \left(\frac{1}{2}v_M^2 + (1 + \gamma)U_{M,\text{ext}} + (\mathbf{v}_M \cdot \dot{\boldsymbol{\mathcal{X}}}) \right) \dot{\boldsymbol{\mathcal{X}}} + \frac{1}{2}(\mathbf{v}_M \cdot \dot{\boldsymbol{\mathcal{X}}})\mathbf{v}_M \right\}_{\text{TL}} + \mathcal{O}(7.82 \times 10^{-9} \text{ m/s}), \quad (\text{A26})$$

$$\begin{aligned} (\ddot{\mathbf{x}} - \ddot{\mathbf{x}}_M)_{\text{TDB}} = & \ddot{\boldsymbol{\mathcal{X}}}_{\text{TL}} + (L_B - L_L)\ddot{\boldsymbol{\mathcal{X}}}_{\text{TL}} - c^{-2} \left\{ \left(v_M^2 + (2 + \gamma)U_{M,\text{ext}} + 3(\mathbf{a}_M \cdot \boldsymbol{\mathcal{X}}) + 2(\mathbf{v}_M \cdot \dot{\boldsymbol{\mathcal{X}}}) \right) \ddot{\boldsymbol{\mathcal{X}}} + \right. \\ & + \left((\mathbf{v}_M \cdot \mathbf{a}_M) + (1 + 2\gamma)\dot{U}_{M,\text{ext}} + 4(\mathbf{a}_M \cdot \dot{\boldsymbol{\mathcal{X}}}) + (\mathbf{v}_M \cdot \ddot{\boldsymbol{\mathcal{X}}}) \right) \dot{\boldsymbol{\mathcal{X}}} + \left((\mathbf{a}_M \cdot \dot{\boldsymbol{\mathcal{X}}}) + \frac{1}{2}(\mathbf{v}_M \cdot \ddot{\boldsymbol{\mathcal{X}}}) \right) \mathbf{v}_M + \\ & \left. + \left((\mathbf{a}_M \cdot \boldsymbol{\mathcal{X}}) + (\mathbf{v}_M \cdot \dot{\boldsymbol{\mathcal{X}}}) - (\dot{\boldsymbol{\mathcal{X}}} \cdot \dot{\boldsymbol{\mathcal{X}}}) - (\boldsymbol{\mathcal{X}} \cdot \ddot{\boldsymbol{\mathcal{X}}}) \right) \mathbf{a}_M + (\mathbf{a}_M \cdot \ddot{\boldsymbol{\mathcal{X}}})\boldsymbol{\mathcal{X}} \right\}_{\text{TL}} + \mathcal{O}(3.99 \times 10^{-15} \text{ m/s}^2), \quad (\text{A27}) \end{aligned}$$

where $\mathbf{v}_M = d\mathbf{x}_M/dt$, $\mathbf{a}_M = d^2\mathbf{x}_M/dt^2$, and $U_{M,\text{ext}}$ and $\dot{U}_{M,\text{ext}}$ are given by (19) and (30), correspondingly by replacing E with M, see [21]. Also, the error terms are determined by the magnitude of similar terms as in (36), (42), and (51).

As a result, for cislunar GNSS use, retain Eqs. (A25)–(A27) with the same screening thresholds adopted in Sec. II D (positions: 7×10^{-5} m, velocities: 1.3×10^{-7} m/s, accelerations: 6.7×10^{-14} m/s²). The scale term $(L_B - L_L)\boldsymbol{\mathcal{X}}_{\text{TL}}$ and the Lorentz contraction $\frac{1}{2}c^{-2}(\mathbf{v}_M \cdot \boldsymbol{\mathcal{X}})\mathbf{v}_M$ dominate the position transformations; the largest periodic term in (TL – TT) is $\approx 0.473 \mu\text{s}$ at the lunar sidereal period (A23).

⁴ Note that these expressions are analogous to those developed for the GCRS in (36), (42), and (51), respectively.